

Randomized Kaczmarz Methods with Beyond-Krylov Convergence*

Michał Dereziński[†] Deanna Needell[‡] Elizaveta Rebrova[§] Jiaming Yang[¶]

January 22, 2025

Abstract

Randomized Kaczmarz methods form a family of linear system solvers which converge by repeatedly projecting their iterates onto randomly sampled equations. While effective in some contexts, such as highly over-determined least squares, Kaczmarz methods are traditionally deemed secondary to Krylov subspace methods, since this latter family of solvers can exploit outliers in the input’s singular value distribution to attain fast convergence on ill-conditioned systems.

In this paper, we introduce Kaczmarz++, an accelerated randomized block Kaczmarz algorithm that exploits outlying singular values in the input to attain a fast Krylov-style convergence. Moreover, we show that Kaczmarz++ captures large outlying singular values provably faster than popular Krylov methods, for both over- and under-determined systems. We also develop an optimized variant for positive semidefinite systems, called CD++, demonstrating empirically that it is competitive in arithmetic operations with both CG and GMRES on a collection of benchmark problems. To attain these results, we introduce several novel algorithmic improvements to the Kaczmarz framework, including adaptive momentum acceleration, Tikhonov-regularized projections, and a memoization scheme for reusing information from previously sampled equation blocks.

*This work was funded by NSF grant CCF-2338655 (MD and JY), NSF grant DMS-2408912 (DN), and NSF grant DMS-2309685 (ER).

[†]University of Michigan (derezin@umich.edu)

[‡]University of California, Los Angeles (deanna@math.ucla.edu)

[§]Princeton University (elre@princeton.edu)

[¶]University of Michigan (jiamyang@umich.edu)

Contents

1	Introduction	3
1.1	Overview of the Main Algorithm	5
1.2	Related work	7
1.3	Notation	8
1.4	Organization	8
2	Stable Convergence with Adaptive Acceleration	8
3	Sharp Convergence Rate via Regularized Projections	11
3.1	Expectation of the Regularized Projection	11
3.2	Variance of the Regularized Projection	14
4	Optimized Computations via Block Memoization	15
4.1	Computing the Projection Step	15
4.2	Block Memoization	17
4.3	Overall Computational Analysis	19
5	Improved Algorithm for Positive Semidefinite Systems	20
5.1	Coordinate Descent	20
5.2	Simplified Block Memoization	20
5.3	Symmetric Randomized Hadamard Transform	21
5.4	Error Estimation and Adaptive Tuning	22
6	Numerical Experiments	23
6.1	Experimental Setup	24
6.2	Verifying Our Convergence Analysis	24
6.3	Comparison with Krylov Subspace Methods	26
7	Conclusions	27
A	Acceleration Analysis: Proofs of Lemmas 2.3 and 2.4	31
A.1	Proof of Lemma 2.3	31
A.2	Proof of Lemma 2.4	33
B	Regularized DPPs: Proof of Lemma 3.6	34
C	Analysis of SymFHT: Proof of Theorem 5.1	34
D	Further Numerical Experiments	36
D.1	Testing Acceleration and Block Memoization	36
D.2	Comparison with Krylov Subspace Methods	39
D.3	Testing Regularization in Projection	41

1 Introduction

The Kaczmarz method [Kac37] is an iterative algorithm for solving large linear systems of equations, which has found many applications [Nat01, FCM⁺92, HM93] due to its simple and memory-efficient updates that operate on a single equation at a time. Numerous variants of this method have been studied, most notably incorporating randomized equation selection to enable rigorous convergence analysis (Randomized Kaczmarz, [SV09]), as well as block updates [Elf80, NT14] that operate on multiple equations at a time to better balance memory and computations. Notably, Randomized Kaczmarz can be viewed as an instance of Stochastic Gradient Descent (SGD), and this connection has led to weighted sampling schemes for SGD [NWS14].

Kaczmarz(-type) methods have proven effective when the linear system is highly over-determined and the computing environment restricts access to the input data, thus benefiting from their cheap and localized updates. However, the popular belief is that, outside of these considerations, Krylov subspace methods such as Conjugate Gradient (CG) [HS52], LSQR [PS82], and GMRES [SS86] are typically superior to Kaczmarz methods on account of their ability to exploit outliers in the input’s singular value distribution, attaining fast convergence even for some highly ill-conditioned systems [AL86]. In this work, we re-examine this assertion, developing Kaczmarz methods that can similarly exploit outlying singular values in the input to achieve fast convergence, going even beyond what Krylov subspace methods can attain for a natural class of singular value distributions. Crucially, our proposed methods do not require the systems to be very tall or even over-determined to work well.

To achieve this beyond-Krylov convergence, we develop Kaczmarz++, a randomized block Kaczmarz method that incorporates several novel algorithmic techniques: adaptive acceleration, regularized projections, and block memoization. Illustrating our claims, let us focus first on solving a square $n \times n$ linear system $\mathbf{A}\mathbf{x} = \mathbf{b}$ for $\mathbf{A} \in \mathbb{R}^{n \times n}$ and $\mathbf{b} \in \mathbb{R}^n$, but extensions to rectangular under- and over-determined systems are provided in the later sections. Given $1 \leq k \leq n$, we show that Kaczmarz++ with block size proportional to k solves such a system to within ϵ error in:

$$\text{(Kaczmarz++, Thm. 4.5)} \quad \underbrace{\tilde{O}(n^2 + nk^2)}_{\text{Phase 1}} + \underbrace{\tilde{O}(n^2 \bar{\kappa}_k \log 1/\epsilon)}_{\text{Phase 2}} \quad \text{operations}, \quad (1.1)$$

where \tilde{O} hides logarithmic factors described in detail alongside the theorem, while $\bar{\kappa}_k$ is the normalized Demmel condition number of the matrix \mathbf{A} excluding the top- k part of its singular value decomposition (SVD):

$$\bar{\kappa}_k := \bar{\kappa}(\mathbf{A} - \mathbf{A}_k), \quad \text{for} \quad \bar{\kappa}(\mathbf{M}) := \|\mathbf{M}\|_F \|\mathbf{M}^\dagger\| / \sqrt{\text{rank}(\mathbf{M})}. \quad (1.2)$$

Here, $\mathbf{A}_k = \sum_{i=1}^k \sigma_i \mathbf{u}_i \mathbf{v}_i^\top$ denotes the top- k part of \mathbf{A} ’s SVD, and $\|\cdot\|_F$ is the matrix Frobenius norm. Demmel condition number $\|\mathbf{M}\|_F \|\mathbf{M}^\dagger\| = \|\mathbf{M}\|_F / \sigma_{\min}^+(\mathbf{M})$ is often used to describe the convergence rate of Kaczmarz methods, starting from [SV09], and when normalized by $\sqrt{\text{rank}(\mathbf{M})}$, it is always upper-bounded by the classical condition number $\kappa(\mathbf{M}) := \|\mathbf{M}\| \|\mathbf{M}^\dagger\|$.

As suggested by (1.1), Kaczmarz++ exhibits two phases of convergence: In the first phase, the algorithm implicitly *captures the top- k part of \mathbf{A} ’s spectrum* via our block memoization scheme that requires only $\tilde{O}(nk)$ additional memory. Then, in the second phase, it uses this information (along with our adaptive acceleration scheme) to attain a convergence rate that is *independent of the top- k singular values of \mathbf{A}* .

To put this result in context, consider a comparable convergence guarantee achievable by a Krylov subspace method (such as LSQR) for solving a dense $n \times n$ ill-conditioned linear system with k large outlying singular values. Such a method is also expected to exhibit two phases of

convergence, where the first phase builds the Krylov subspace that captures the top- k part of \mathbf{A} 's SVD, while the second phase leverages it to attain fast convergence, reaching ϵ error after:

$$\text{(Krylov, e.g., [AL86])} \quad \underbrace{O(n^2k)}_{\text{Phase 1}} + \underbrace{O(n^2\kappa_k \log 1/\epsilon)}_{\text{Phase 2}} \quad \text{operations.} \quad (1.3)$$

Here, $\kappa_k := \kappa(\mathbf{A} - \mathbf{A}_k)$ is the condition number of \mathbf{A} excluding its top- k singular values.

There are two key differences between the guarantees (1.1) and (1.3). First, the fast convergence of Kaczmarz++ relies on $\bar{\kappa}_k$, which can be substantially smaller than κ_k . Second, and more importantly, the first phase of Kaczmarz++ takes only $\tilde{O}(n^2 + nk^2)$ time, which is much more efficient than the $O(n^2k)$ first phase of Krylov when k is sufficiently larger than a constant (and smaller than n). This is because building the Krylov subspace for the outlying singular values requires at least k matrix-vector products with the full matrix \mathbf{A} , whereas in the initial phase of Kaczmarz++, the algorithm iterates over $\tilde{O}(n/k)$ blocks of $\tilde{O}(k)$ rows each, a computational equivalent of only a few matrix-vector products.

Naturally, the above guarantees do not provide a complete convergence comparison between Kaczmarz++ and Krylov subspace methods (e.g., they do not account for *small* outlying singular values). However, they indicate that Kaczmarz methods can be competitive with Krylov solvers in terms of arithmetic operations even for square linear systems, and not only for highly over-determined ones, as is often suggested. To verify this claim empirically, we develop a practical implementation of Kaczmarz++ that is specifically optimized for positive semidefinite systems (CD++, Algorithm 3), and test it on a collection of benchmark problems from the machine learning literature [VvRBT13, PVG⁺11], which are known to exhibit large outlying eigenvalues. The experiments confirm our theoretical findings, showing that our algorithm is competitive in floating point operations with both CG and GMRES on a range of input matrices.

Main contributions. As part of Kaczmarz++, we introduce several novel algorithmic techniques to the broader Kaczmarz toolbox, which are crucial both for the convergence analysis and the numerical performance.

1. *Adaptive acceleration:* We propose a new way of introducing Nesterov's momentum into Kaczmarz updates, which is both stable with respect to its hyper-parameters and can be adaptively tuned during runtime (Section 2).
2. *Regularized projections:* We add Tikhonov regularization to the classical Kaczmarz projection steps, showing that it not only makes them better-conditioned, but also reduces the variance coming from randomization, enabling our convergence analysis (Section 3).
3. *Block memoization:* Our algorithm saves and reuses small Cholesky factors associated with the sampled equation blocks, thereby speeding up subsequent iterations in the second phase of the convergence, while at the same time maintaining a low memory footprint (Section 4).
4. *Symmetric Hadamard transform:* A key step in our algorithm is to preprocess the linear system with a randomized Hadamard transform. As an auxiliary result, we give a new recursive scheme for applying the Hadamard transform to symmetric matrices which reduces arithmetic operations by half (Section 5).

1.1 Overview of the Main Algorithm

In this section, we motivate and derive our Kaczmarz++ algorithm, describing how the simultaneous use of fast preprocessing, adaptive acceleration, regularized projections, and block memoization enable it to achieve the claimed convergence guarantees.

Consider solving a consistent linear system with m equations, $\mathbf{A}\mathbf{x} = \mathbf{b}$, where $\mathbf{A} \in \mathbb{R}^{m \times n}$ and $\mathbf{b} \in \mathbb{R}^m$. The classical block Kaczmarz method constructs a sequence of iterates $\mathbf{x}_0, \mathbf{x}_1, \dots$ by repeatedly choosing a subset $S = S(t) \subseteq \{1, \dots, m\} =: [m]$ of those equations, and then projecting the current iterate \mathbf{x}_t onto the subspace of solutions of those equations, i.e., the under-determined system $\mathbf{A}_S \mathbf{x} = \mathbf{b}_S$. This leads to the block Kaczmarz update which can be stated as follows:

$$\mathbf{x}_{t+1} = \underset{\mathbf{x}: \mathbf{A}_S \mathbf{x} = \mathbf{b}_S}{\operatorname{argmin}} \|\mathbf{x} - \mathbf{x}_t\|^2 = \mathbf{x}_t - \mathbf{A}_S^\dagger (\mathbf{A}_S \mathbf{x}_t - \mathbf{b}_S).$$

Randomized preprocessing. Effective selection of the subset S in each iteration is crucial for obtaining fast convergence of the block Kaczmarz method, and randomization has been suggested as an effective strategy to diversify the selection process. Here, one approach, following the original Randomized Kaczmarz method [SV09], is to use importance sampling that emphasizes equations with large row norms. However, it has proven difficult to characterize the correct importance weights that ensure provably fast convergence of block Kaczmarz. So, we opt for a different strategy: preprocessing the linear system using a Randomized Hadamard Transform [AC09, Tro11].

Definition 1.1. An $m \times m$ randomized Hadamard transform (RHT) is a matrix $\mathbf{Q} = \mathbf{H}\mathbf{D}$, where \mathbf{H} is the Hadamard matrix and \mathbf{D} is an $m \times m$ diagonal matrix with random $\pm 1/\sqrt{m}$ entries. Applying \mathbf{Q} to a vector takes $m \log m$ arithmetic operations.

We note that the Hadamard matrix, similarly to a Discrete Fourier Transform (DFT), is a scaled orthogonal matrix (specifically, $\mathbf{H}^\top \mathbf{H} = m\mathbf{I}_m$) that admits fast matrix-vector multiply (see Appendix C for a detailed discussion). In fact, these are the only two properties we use in our analysis, and one could replace Hadamard with a DFT or other fast transforms.

Since $\mathbf{Q}^\top \mathbf{Q} = \mathbf{I}$, transforming the system $\mathbf{A}\mathbf{x} = \mathbf{b}$ into $\mathbf{Q}\mathbf{A}\mathbf{x} = \mathbf{Q}\mathbf{b}$ does not affect the solution of the system nor does it affect the singular value distribution of the input matrix. However, crucially, it ensures that all equations become roughly equally important (this is known as *incoherence*), which allows us to select a representative subset S uniformly at random. Using the fast matrix-vector multiply, this transformation can be done using $mn \log m$ arithmetic operations. This preprocessing step, while essential for parts of our analysis, may be skipped when the input matrix naturally exhibits an incoherence property [NT14].

Regularized projections. Even after preprocessing with the RHT (and especially if this is omitted), a randomly selected sub-matrix \mathbf{A}_S may be poorly conditioned, which adversely affects the performance of block Kaczmarz, especially if one chooses to solve the block system using an iterative method. To guard against this, instead of the true projection step, we consider a *regularized* projection, defined as the following regularized least squares problem:

$$\begin{aligned} \mathbf{x}_{t+1} &= \underset{\mathbf{x} \in \mathbb{R}^n}{\operatorname{argmin}} \left\{ \|\mathbf{A}_S \mathbf{x} - \mathbf{b}_S\|^2 + \lambda \|\mathbf{x} - \mathbf{x}_t\|^2 \right\} \\ &= \mathbf{x}_t - \mathbf{A}_S^\top (\mathbf{A}_S \mathbf{A}_S^\top + \lambda \mathbf{I})^{-1} (\mathbf{A}_S \mathbf{x}_t - \mathbf{b}_S) =: \mathbf{x}_t - \mathbf{w}_t. \end{aligned} \tag{1.4}$$

Note that by letting $\lambda = 0$, this formulation recovers standard block Kaczmarz, however a positive λ ensures that the sub-problem being solved is not too ill-conditioned. This plays a crucial role in the convergence analysis of our method (see Section 3), and it also improves the stability of solving the sub-problem (see Section 4).

Block memoization. Even with the regularization, the cost of the projection step in each iteration of Kaczmarz++ is still a substantial computational bottleneck, as it requires computing or approximately applying the inverse of $\mathbf{A}_S \mathbf{A}_S^\top + \lambda \mathbf{I}$, e.g., via its Cholesky factor, $\mathbf{R} = \text{chol}(\mathbf{A}_S \mathbf{A}_S^\top + \lambda \mathbf{I})$. In Section 4.1, we make the projection steps even more efficient by computing an approximation of the Cholesky factor, $\tilde{\mathbf{R}} \approx \mathbf{R}$, and combining this with an inner solver. Finally, to further amortize these costs over the entire convergence run of the algorithm, we store and reuse the Cholesky factors computed in early iterations via what we refer to as *block memoization*.

To enable block memoization, it is crucial that the algorithm draws its blocks from a small collection \mathcal{B} of previously sampled block sets, so that we can reuse a previously computed Cholesky factor $\tilde{\mathbf{R}}[S]$ for a set $S \in \mathcal{B}$. However, this comes with a trade-off: we should expect the convergence rate attained by the algorithm to get worse as we restrict the method to a smaller collection of blocks. Fortunately, we show in Section 4.2 that when using blocks of size $\tilde{O}(k)$, it suffices to sample a collection \mathcal{B} of $\tilde{O}(\frac{m}{k})$ random blocks, which can then be continually reused while retaining the same convergence guarantees as if we sampled fresh random blocks at every step. This scheme requires only $\tilde{O}(mk)$ additional memory for storing the Cholesky factors.

Adaptive acceleration. A key limitation of the Kaczmarz update is that it does not accumulate any information about the trajectory of its convergence, which could be used to accelerate it. This stands in contrast to, for instance, Krylov methods such as CG, as well as momentum-based methods such as accelerated gradient descent (AGD), which use the information from all previous update directions to construct the next step. To address this, we develop a new way of introducing momentum into the block Kaczmarz update through a careful reformulation of Nesterov’s momentum that is both theoretically principled and practically effective.

To explain how we accelerate block Kaczmarz using momentum, we first describe the AGD algorithm, following Nesterov [Nes13]. In the context of solving a linear system, AGD can be viewed as minimizing the convex quadratic $f(\mathbf{x}) = \frac{1}{2} \mathbf{x}^\top \mathbf{A}^\top \mathbf{A} \mathbf{x} - \mathbf{x}^\top \mathbf{A}^\top \mathbf{b}$, via the iterative update $\mathbf{x}_{t+1} = \mathbf{x}_t - \mathbf{w}_t + \mathbf{m}_{t+1}$, where $\mathbf{w}_t = \alpha \nabla f(\mathbf{x}_t)$ is the gradient step, and \mathbf{m}_t is the momentum step:

$$\mathbf{m}_{t+1} = \frac{1 - \rho}{1 + \rho} (\mathbf{m}_t - \mathbf{w}_t), \quad \rho \in [0, 1]. \quad (1.5)$$

We note that the above scheme is precisely the AGD scheme (2.2.11) in [Nes13], obtained by substituting their y_k with our \mathbf{x}_t , initializing $\mathbf{m}_0 = \mathbf{0}$, and setting $\alpha = 1/L$, $\rho = \sqrt{\mu/L}$ using their μ and L . Here, parameter ρ is also the theoretical convergence rate of AGD: one can show that $\|\mathbf{x}_t - \mathbf{x}^*\|^2 \leq C(1 - \rho)^t \|\mathbf{x}_0 - \mathbf{x}^*\|^2$ for an appropriate problem-dependent $C > 0$ (Theorem 2.2.3 in [Nes13]).

Based on these observations, we replicate the above acceleration procedure for block Kaczmarz, by setting \mathbf{w}_t in the momentum recursion (1.5) to be the regularized projection step (1.4), and adjusting ρ to be the target convergence rate of our method. However, this does not fully take into account the stochasticity of the block Kaczmarz update, which operates only on a fraction of the matrix \mathbf{A} at a time. This forces us to curb the momentum step further, by introducing an additional step size η , which should be proportional to the ratio between the block size and the rank of \mathbf{A} :

$$\mathbf{x}_{t+1} = \mathbf{x}_t - \mathbf{w}_t + \eta \mathbf{m}_{t+1}, \quad \eta \in [0, 1].$$

In Section 2, we show that the above accelerated update is remarkably stable with respect to both η and ρ . Further, motivated by this analysis, in Section 5 we propose an adaptive scheme that periodically updates ρ at runtime using the current estimate of the convergence rate of the

algorithm. We observe that this mechanism exhibits a self-correcting feedback loop that quickly arrives at a near-optimal convergence.

Combining the above ideas, we obtain Kaczmarz++ (Algorithm 1). Building on this, in Section 5 we propose CD++ (Algorithm 3), a coordinate descent-type algorithm derived out of Kaczmarz++, which is optimized for positive definite systems.

Algorithm 1 Kaczmarz++

- 1: **Input:** $\mathbf{A} \in \mathbb{R}^{m \times n}$, $\mathbf{b} \in \mathbb{R}^n$, block size s , iterate \mathbf{x}_0 , parameters B, λ, ρ, η ;
 - 2: Initialize $\mathbf{m}_0 \leftarrow \mathbf{0}$;
 - 3: Compute $\mathbf{A} \leftarrow \mathbf{Q}\mathbf{A}$ and $\mathbf{b} \leftarrow \mathbf{Q}\mathbf{b}$; ▷ Preprocessing with RHT \mathbf{Q} .
 - 4: Sample $\mathcal{B} \leftarrow \{S_1, S_2, \dots, S_B\}$ where $S_i \sim \binom{[m]}{s}$; ▷ Prepare B index subsets.
 - 5: **for** $t = 0, 1, \dots$ **do**
 - 6: Draw a random S from \mathcal{B} ;
 - 7: **if** $\tilde{\mathbf{R}}[S] = \text{null}$ **then** $\tilde{\mathbf{R}}[S] \approx \text{chol}(\mathbf{A}_S \mathbf{A}_S^\top + \lambda \mathbf{I})$; ▷ Save Cholesky factor.
 - 8: $\tilde{\mathbf{w}}_t \approx \mathbf{A}_S^\top (\mathbf{A}_S \mathbf{A}_S^\top + \lambda \mathbf{I})^{-1} (\mathbf{A}_S \mathbf{x}_t - \mathbf{b}_S)$ using $\tilde{\mathbf{R}}[S]$; ▷ Regularized projection.
 - 9: $\mathbf{m}_{t+1} \leftarrow \frac{1-\rho}{1+\rho} (\mathbf{m}_t - \tilde{\mathbf{w}}_t)$; ▷ Nesterov momentum.
 - 10: $\mathbf{x}_{t+1} \leftarrow \mathbf{x}_t - \tilde{\mathbf{w}}_t + \eta \mathbf{m}_{t+1}$; ▷ Kaczmarz++ update.
 - 11: Revise convergence rate estimate ρ ; ▷ Adaptive acceleration.
 - 12: **end for**
 - 13: **return** $\tilde{\mathbf{x}} = \mathbf{x}_t$; ▷ Solves $\mathbf{A}\mathbf{x} = \mathbf{b}$.
-

1.2 Related work

The block Kaczmarz method was first introduced by [Elf80], motivated by applications in image reconstruction [EHL81]. Later, a randomized implementation of block Kaczmarz was developed and analyzed by [NT14], who showed that under some assumptions on the row-norms and spectral norm of the input matrix, after preprocessing it with a randomized Hadamard transform, a sufficiently large random partition of an $n \times n$ linear system into n/s blocks of size s leads to a convergent block Kaczmarz method. However, even if we ignore their assumptions on the input matrix (which are not needed in our work), those convergence guarantees scale with the squared condition number $\kappa^2(\mathbf{A})$, and thus do not exploit the singular value distribution as shown in (1.1).

An alternative block-construction strategy, first proposed by [GR15], is to transform the matrix \mathbf{A} via a random *sketching* matrix $\mathbf{\Pi} \in \mathbb{R}^{s \times n}$, so that $\mathbf{\Pi}\mathbf{A}$ is no longer a subset of equations, but rather a collection of linear combinations of equations. A simple choice is to use a Gaussian matrix or a sparse random sign matrix $\mathbf{\Pi}$. These approaches offer a finer control on the quality of sampled blocks, but at the expense of substantially larger cost, since one must compute a new sketch $\mathbf{\Pi}\mathbf{A}$ at every iteration of the algorithm. [RN21] were the first to characterize the convergence rate of Block Kaczmarz with Gaussian sketches, however their convergence also scales with $\kappa^2(\mathbf{A})$ and does not exploit outlying singular values. In [RN21], a sketch memoization idea was also proposed, in the form of sampling from a set of precomputed sketches, although they require as many as $\tilde{O}(n^2)$ precomputed sketches to ensure convergence.

Recently, there has been a number of works suggesting that variants of block Kaczmarz can exploit k large outliers in the singular value distribution, by expressing its convergence in terms of $\bar{\kappa}_k$ or κ_k . [DR24] were the first to show this, however due to the large cost of Gaussian sketching and lack of acceleration, their method does not have a computational benefit over existing approaches. Then, [DY24] showed that a similar convergence guarantee can be obtained by block Kaczmarz with uniformly sampled blocks, after RHT preprocessing. Their algorithm converges in $\tilde{O}(n^2 +$

$nk^2\bar{\kappa}_k^2 \log 1/\epsilon$) operations. Most recently, [DLNR24] obtained $\tilde{O}((n^2 + nk^2)\kappa_k \log 1/\epsilon)$ operations by introducing momentum acceleration via the scheme of [GHR18], but at the expense of relying on sparse sketching for block construction (much slower than uniform sampling).

An alternative variant of block Kaczmarz that exploits large outlying singular values was recently proposed in [LR24]. This algorithm first finds a subsystem spanning the leading subspace of the system, and then projects future iterates onto its solution subspace. However, this method requires some external knowledge about the leading subspace to attain a computational advantage over the other approaches. Several other recently developed Kaczmarz methods [ALM24, EGW24, PJM23] introduce acceleration and/or adaptivity, but do not provably exploit large outlying singular values.

Our Kaczmarz++, which requires $\tilde{O}(nk^2 + n^2\bar{\kappa}_k \log 1/\epsilon)$ operations to converge, improves on all of these recent prior results in two primary ways: 1) It is the only one to achieve the correct condition number dependence, scaling with $\bar{\kappa}_k$ as opposed to $\bar{\kappa}_k^2$ or κ_k ; and 2) It is the only block Kaczmarz method to exhibit two distinct phases of convergence, in the sense that the $\tilde{O}(n^2 + nk^2)$ cost of learning the outlying singular values is not incurred for the entire $\tilde{O}(\bar{\kappa}_k \log 1/\epsilon)$ length of the convergence. This improvement, a result of our block memoization scheme and its analysis, allows Kaczmarz++ to always match or improve upon the Krylov convergence guarantee (1.3).

1.3 Notation

We let $[m] := \{1, \dots, m\}$, whereas $\binom{[m]}{s}$ denotes all size s subsets of $[m]$. For a matrix $\mathbf{A} \in \mathbb{R}^{m \times n}$ and subset $S \in \binom{[m]}{s}$, we use $\mathbf{A}_S \in \mathbb{R}^{s \times n}$ to denote the submatrix of the rows of \mathbf{A} indexed by S , and if $m = n$, then $\mathbf{A}_{S,S} \in \mathbb{R}^{s \times s}$ is the principal submatrix indexed by S . We use $\|\mathbf{A}\|$, $\|\mathbf{A}\|_F$, and \mathbf{A}^\dagger to denote the spectral/Frobenius norms of matrix \mathbf{A} as well as its Moore-Penrose pseudoinverse, while $\lambda_{\max}(\mathbf{A})$ and $\lambda_{\min}^+(\mathbf{A})$ are the largest and smallest positive eigenvalues of an $n \times n$ positive semidefinite (PSD) matrix, denoted $\mathbf{A} \in \mathcal{S}_n^+$. For $\mathbf{A} \in \mathcal{S}_n^+$ and $\mathbf{v} \in \mathbb{R}^n$, we use $\|\mathbf{v}\|_{\mathbf{A}} = \sqrt{\mathbf{v}^\top \mathbf{A} \mathbf{v}}$, and for symmetric matrices, $\mathbf{A} \preceq \mathbf{B}$ means that $\mathbf{B} - \mathbf{A} \in \mathcal{S}_n^+$. We use $C > 0$ to denote an absolute constant, which may change from line to line.

1.4 Organization

In Section 2 we perform the convergence analysis of our accelerated Kaczmarz update as a function of the randomized block selection, verifying its stability with respect to the momentum parameters ρ and η . Then, in Section 3 we characterize the convergence rate under uniform block sampling after RHT, in terms of the regularizer λ . In Section 4, we introduce and analyze block memoization, together with a discussion of the overall computational cost of Kaczmarz++. Finally, Section 5 describes our specialized CD++ algorithm for positive semidefinite linear systems, and Section 6 has numerical experiments. We give conclusions in Section 7.

2 Stable Convergence with Adaptive Acceleration

In this section, we establish how the convergence of Kaczmarz++ (Algorithm 1) depends on the properties of the randomized block selection scheme. This guarantee does *not* assume that the system was preprocessed with a Randomized Hadamard Transform. Moreover, it applies to all consistent linear systems, regardless of aspect ratio, and most block sampling schemes. Main theoretical result of this section is the following theorem:

Theorem 2.1 (General convergence rate). *Given $\mathbf{A} \in \mathbb{R}^{m \times n}$ and $\mathbf{b} \in \mathbb{R}^n$, let \mathbf{x}^* be the minimum-norm solution to $\mathbf{A}\mathbf{x} = \mathbf{b}$. Also, let \mathcal{D} be a probability distribution over subsets of $[m]$. Given $\lambda \geq 0$, define the random regularized projection:*

$$\mathbf{P}_{\lambda,S} := \mathbf{A}_S^\top (\mathbf{A}_S \mathbf{A}_S^\top + \lambda \mathbf{I})^\dagger \mathbf{A}_S, \quad S \sim \mathcal{D},$$

and suppose that $\bar{\mathbf{P}}_\lambda := \mathbb{E}[\mathbf{P}_{\lambda,S}]$ has the same null space as \mathbf{A} . Define the following:

$$\begin{aligned} \mu &:= \mu(\mathbf{A}, \mathcal{D}, \lambda) = \lambda_{\min}^+(\bar{\mathbf{P}}_\lambda), \\ \nu &:= \nu(\mathbf{A}, \mathcal{D}, \lambda) = \lambda_{\max}\left(\mathbb{E}[(\bar{\mathbf{P}}_\lambda^{\dagger/2} \mathbf{P}_{\lambda,S} \bar{\mathbf{P}}_\lambda^{\dagger/2})^2]\right), \\ \text{and } \bar{\rho} &:= \bar{\rho}(\mathbf{A}, \mathcal{D}, \lambda) = \sqrt{\frac{\mu}{\nu}}. \end{aligned} \tag{2.1}$$

Let $\rho \in [0, c\bar{\rho}]$ and $\eta \in [\frac{c}{\nu}, \frac{1}{2\nu}]$ for some $c \in (0, 1/2]$, and suppose that a sequence \mathbf{x}_t is updated as in lines 6-10 of Algorithm 1, allowing the regularized projection step (line 8) to be computed inexactly, returning $\tilde{\mathbf{w}}_t$ such that $\|\tilde{\mathbf{w}}_t - \mathbf{w}_t\| \leq \frac{\rho^2}{8\eta} \|\mathbf{w}_t\|$. Then,

$$\mathbb{E}\left[\|\mathbf{x}_t - \mathbf{x}^*\|^2\right] \leq 8(1 - \rho/2)^t \cdot \|\mathbf{x}_0 - \mathbf{x}^*\|^2.$$

Remark 2.2 (Stability). *Assuming exact projection steps, it is possible to get convergence rate $8(1 - \sqrt{\mu/\nu})^t$ by setting $\rho = \bar{\rho}$ and $\eta = \frac{1/\nu - \bar{\rho}}{1 - \bar{\rho}}$, replicating the convergence rate achieved by an acceleration scheme of [GHR18].*

However, a key feature of our algorithm captured by Theorem 2.1 is that our proposed acceleration (momentum) scheme for block Kaczmarz is remarkably stable with respect to both the choice of parameters ρ and η , as well as the precision of solving the regularized projection step. Specifically, as one cannot hope to find the parameters at runtime, our result shows that it suffices to use an over-estimate of ν and an under-estimate of $\bar{\rho}$, where the estimation accuracy is captured by a factor c .

We highlight this stability as a key feature of our scheme, since it motivates our adaptive acceleration tuning for parameter ρ , described later in Section 5. Further, in Section 3, we show that after preprocessing with the RHT, ν can be bounded by $\tilde{O}(\frac{m}{s})$, where s is the block size, which suggests a simple problem-agnostic estimate for η as well. Finally, we also show similar stability guarantees with respect to the regularization parameter λ in Section 3.

Our next goal is to prove Theorem 2.1. We obtain this result through a careful reformulation of the Kaczmarz++ update, replacing the momentum vector with two auxiliary iterate sequences, which allows us to lean on existing Lyapunov-style convergence analysis for accelerated methods [GHR18]. Instead of maintaining the momentum vector \mathbf{m}_t , we initialize $\mathbf{v}_0 = \mathbf{y}_0$ and maintain iterates $\mathbf{x}_t, \mathbf{y}_t, \mathbf{v}_t$ based on the following update rules:

$$\begin{cases} \mathbf{x}_t = \alpha \mathbf{v}_t + (1 - \alpha) \mathbf{y}_t \\ \text{Compute } \tilde{\mathbf{w}}_t \approx \mathbf{w}_t \\ \mathbf{y}_{t+1} = \mathbf{x}_t - \tilde{\mathbf{w}}_t \\ \mathbf{v}_{t+1} = \beta \mathbf{v}_t + (1 - \beta) \mathbf{x}_t - \gamma \tilde{\mathbf{w}}_t \end{cases} \tag{2.2}$$

These iterates are essentially in the form considered earlier in [GHR18, DLNR24], and we can carry out the analysis of Nesterov's acceleration similarly, with the key difference that we use regularized projections in the Kaczmarz update, whereas prior works use exact projections. This results in the following estimate for the convergence rate in a convenient metric Δ_t as defined below and under a particular parameter choice.

Lemma 2.3 (Based on [GHR18, Lem. 2, Thm. 3]). *In the setting of Theorem 2.1, observe that $\mu := \lambda_{\min}^+(\bar{\mathbf{P}}_\lambda)$ and $\nu := \lambda_{\max}(\mathbb{E}[(\bar{\mathbf{P}}_\lambda^{\dagger/2} \mathbf{P}_{\lambda,S} \bar{\mathbf{P}}_\lambda^{\dagger/2})^2])$ satisfy $1 \leq \nu \leq 1/\mu$. Moreover, suppose that $\tilde{\mu} \leq \mu$ and $\tilde{\nu} \geq \nu$, and let $\mathbf{x}_t, \mathbf{y}_t, \mathbf{v}_t$ be defined as in (2.2) with $\beta = 1 - \sqrt{\tilde{\mu}/\tilde{\nu}}$, $\gamma = 1/\sqrt{\tilde{\mu}\tilde{\nu}}$ and $\alpha = 1/(1 + \gamma\tilde{\nu})$. Also, let*

$$\Delta_t = \|\mathbf{v}_t - \mathbf{x}^*\|_{\bar{\mathbf{P}}_\lambda^\dagger}^2 + \frac{1}{\tilde{\mu}} \|\mathbf{y}_t - \mathbf{x}^*\|^2.$$

If $\|\tilde{\mathbf{w}}_t - \mathbf{w}_t\| \leq \frac{\tilde{\mu}}{4} \|\mathbf{w}_t\|$, then we have

$$\mathbb{E}[\Delta_{t+1}] \leq \left(1 - \frac{1}{2} \sqrt{\frac{\tilde{\mu}}{\tilde{\nu}}}\right) \cdot \mathbb{E}[\Delta_t].$$

The proof of Lemma 2.3 is generally similar to the proofs of [GHR18, Theorem 3] and [DLNR24, Lemma 23] and it is deferred to Appendix A.1. Next, we prove the equivalence of the Kaczmarz++ update and (2.2).

Lemma 2.4 (Equivalence of two algorithm formulations). *In the notations of Theorem 2.1, let $\rho \in [0, c\bar{\rho}]$ and $\eta \in [\frac{c}{\nu}, \frac{1}{2\nu}]$ for some $c \in (0, 1/2]$. Setting the parameters α, β, γ as in the statement of Lemma 2.3 above with*

$$\tilde{\nu} = \frac{1}{\rho + \eta(1 - \rho)} \quad \text{and} \quad \tilde{\mu} = \rho^2 \tilde{\nu},$$

we will get that (a) $\tilde{\mu} \leq \mu$ and $\tilde{\nu} \geq \nu$; and (b) the iterates \mathbf{x}_t obtained from the updates (2.2), initialized with $\mathbf{v}_0 = \mathbf{y}_0 = \mathbf{x}_0$ and letting $\mathbf{m}_0 = \mathbf{0}$, satisfy

$$\mathbf{m}_{t+1} = \frac{1 - \rho}{1 + \rho} (\mathbf{m}_t - \tilde{\mathbf{w}}_t) \quad \text{and} \quad \mathbf{x}_{t+1} = \mathbf{x}_t - \tilde{\mathbf{w}}_t + \eta \mathbf{m}_{t+1}.$$

That is, the iteration (2.2) will satisfy the assumptions of Lemma 2.3 and it will be equivalent to the lines 6-10 of Algorithm 1.

The proof of this lemma is a direct verification, in particular, checking that $\mathbf{m}_t := \frac{\beta(1-\alpha)}{\gamma-1} (\mathbf{v}_t - \mathbf{y}_t)$ satisfies the above recursion. It is deferred to Appendix A.2.

Proof of Theorem 2.1. By Lemma 2.4, the update from Algorithm 1 is equivalent to the process according to the updates (2.2), with $\alpha = 1/(1 + \sqrt{\tilde{\nu}/\tilde{\mu}}) = \frac{\rho}{1+\rho}$. From Lemma 2.3, we have the following two convergence results in terms of iterates \mathbf{y}_t and \mathbf{v}_t respectively:

$$\begin{cases} \mathbb{E}\|\mathbf{y}_t - \mathbf{x}^*\|^2 \leq \tilde{\mu} \mathbb{E}[\Delta_t] \leq (1 - \rho/2)^t \tilde{\mu} \Delta_0, \\ \mathbb{E}\|\mathbf{v}_t - \mathbf{x}^*\|^2 \leq \mathbb{E}[\Delta_t] \leq (1 - \rho/2)^t \Delta_0, \end{cases} \quad (2.3)$$

where in the second inequality we use that $\bar{\mathbf{P}}_\lambda^\dagger \succeq \mathbf{I}$, thus $\|\mathbf{v}_t - \mathbf{x}^*\| \leq \|\mathbf{v}_t - \mathbf{x}^*\|_{\bar{\mathbf{P}}_\lambda^\dagger}$.

Our goal is to reformulate the convergence result in terms of the sequence \mathbf{x}_t . Since $\mathbf{x}_t = \alpha \mathbf{v}_t + (1 - \alpha) \mathbf{y}_t$, we have the following:

$$\begin{aligned} \mathbb{E}\|\mathbf{x}_t - \mathbf{x}^*\|^2 &= \mathbb{E}\|\alpha(\mathbf{v}_t - \mathbf{x}^*) + (1 - \alpha)(\mathbf{y}_t - \mathbf{x}^*)\|^2 \\ &\leq 2\alpha^2 \mathbb{E}\|\mathbf{v}_t - \mathbf{x}^*\|^2 + 2(1 - \alpha)^2 \mathbb{E}\|\mathbf{y}_t - \mathbf{x}^*\|^2 \\ &\leq 2(1 - \rho/2)^t \left(\alpha^2 \Delta_0 + (1 - \alpha)^2 \tilde{\mu} \Delta_0 \right) \\ &\leq 2(1 - \rho/2)^t (\alpha^2 / \tilde{\mu} + 1) \left(\tilde{\mu} \|\mathbf{y}_0 - \mathbf{x}^*\|_{\bar{\mathbf{P}}_\lambda^\dagger}^2 + \|\mathbf{y}_0 - \mathbf{x}^*\|^2 \right) \\ &\leq 4(1 + 1/\tilde{\nu})(1 - \rho/2)^t \|\mathbf{y}_0 - \mathbf{x}^*\|^2, \end{aligned}$$

where the third step follows from (2.3), the fourth step follows since $\mathbf{v}_0 = \mathbf{y}_0$, the last step follows since $\|\bar{\mathbf{P}}_\lambda^\dagger\| \leq 1/\tilde{\mu}$ and $\alpha = \rho/(1+\rho) < \rho = \sqrt{\tilde{\mu}/\tilde{\nu}}$. Finally, since $\tilde{\nu} \geq \nu \geq 1$ (also by Lemma 2.4) and $\mathbf{x}_0 = \alpha\mathbf{v}_0 + (1-\alpha)\mathbf{y}_0 = \mathbf{y}_0$, we conclude that

$$\mathbb{E}\|\mathbf{x}_t - \mathbf{x}^*\|^2 \leq 4(1+1/\tilde{\nu})(1-\rho/2)^t \|\mathbf{y}_0 - \mathbf{x}^*\|^2 \leq 8(1-\rho/2)^t \cdot \|\mathbf{x}_0 - \mathbf{x}^*\|^2.$$

□

3 Sharp Convergence Rate via Regularized Projections

In the previous section, we showed that, with an appropriate choice of the parameters η and ρ , the convergence rate of Algorithm 1 depends on the theoretical quantity $\bar{\rho} = \sqrt{\mu/\nu}$, where μ and ν are notions of expectation and variance for the random regularized projection $\mathbf{P}_{\lambda,S}$. In this section, we show that after preprocessing with the randomized Hadamard transform, it is possible to give a sharp characterization of both of these quantities in terms of the regularization amount λ and the spectrum of the input matrix \mathbf{A} . First, in Section 3.1, we lower bound the expectation of the regularized projection (with respect to positive semidefinite ordering), which allows us to lower bound the parameter μ . Then we bound the variance of this projection and thus the term ν in Section 3.2. The use of regularization is crucial for bounding ν , and also for the analysis of block memoization in Section 4.

3.1 Expectation of the Regularized Projection

First, we lower bound the parameter $\mu = \lambda_{\min}^+(\mathbb{E}[\mathbf{P}_{\lambda,S}])$ for some $\lambda \geq 0$. Even better, we give a more general result, lower-bounding the entire expectation of the matrix in positive semidefinite ordering, which will be necessary later for the analysis of the variance term ν in Section 3.2.

The following result shows that after applying the randomized Hadamard transform, the expectation of the regularized projection matrix $\mathbf{P}_{\lambda,S}$ based on a random sample of the rows of \mathbf{A} is lower-bounded by an analogously defined regularized projection of the full matrix \mathbf{A} , with appropriately adjusted regularizer (denoted as $\bar{\lambda}$). This result can be viewed as a natural extension of some recent prior works [DY24, DLNR24], which showed such guarantees for classical random projections (i.e., not regularized). While introducing regularization naturally shrinks the random matrix $\mathbf{P}_{\lambda,S}$, and thus it must also decrease the lower bound, we show that there is a level of regularization below which the overall expectation bound does not get significantly affected. Thus, we can reap the benefits of regularization (e.g., when bounding ν later on) without sacrificing any of the effectiveness of the projection.

Theorem 3.1. *Suppose $\mathbf{A} \in \mathbb{R}^{m \times n}$ is transformed by RHT, i.e., $\bar{\mathbf{A}} = \mathbf{Q}\mathbf{A}$. Let $\sigma_1 \geq \sigma_2 \geq \dots$ be \mathbf{A} 's singular values. Given $\delta \in (0, 1)$ and $C \log(m/\delta) \leq k < \text{rank}(\mathbf{A})$, let $\bar{\lambda} = \frac{1}{k} \sum_{i>k} \sigma_i^2$. Let $S \sim \mathcal{U}(m, s)$ be a uniformly random subset of $[m]$ with size $s \geq Ck \log(m\bar{\kappa}_k)$. Then, for any $0 \leq \lambda \leq \frac{k}{m}\bar{\lambda}$, with probability $1 - \delta$ the transformed matrix $\bar{\mathbf{A}}$ satisfies:*

$$\mathbb{E}_{S \sim \mathcal{U}(m,s)} \left[\bar{\mathbf{A}}_S^\top (\bar{\mathbf{A}}_S \bar{\mathbf{A}}_S^\top + \lambda \mathbf{I})^\dagger \bar{\mathbf{A}}_S \right] \succeq \frac{1}{2} \mathbf{A}^\top (\mathbf{A} \mathbf{A}^\top + \bar{\lambda} \mathbf{I})^{-1} \mathbf{A}.$$

Remark 3.2. *Theorem 3.1 implies that after RHT preprocessing, the expected regularized projection has the same null space as \mathbf{A} , and moreover, for any $\lambda \in [0, \frac{k}{m}\bar{\lambda}]$:*

$$\mu\left(\bar{\mathbf{A}}, \mathcal{U}(m, s), \lambda\right) \geq \frac{\sigma_{\min}^+(\mathbf{A})^2/2}{\sigma_{\min}^+(\mathbf{A})^2 + \bar{\lambda}} = \frac{1/2}{1 + \frac{r-k}{k} \bar{\kappa}_k^2} \geq \frac{k}{2r\bar{\kappa}_k^2} \geq \frac{k}{2m\bar{\kappa}_k^2},$$

where r is the rank of \mathbf{A} , while $\bar{\kappa}_k$ and μ are defined in (1.2) and (2.1), respectively.

A similar guarantee to this one was given by [DY24], which was later refined by [DLNR24], however both of these prior results apply only to the case where $\lambda = 0$. Remarkably, the right-hand side in the inequality above is identical to the corresponding Lemma 10 of [DLNR24], which intuitively implies that introducing some regularization into the random projection step of block Kaczmarz does not substantially alter its expectation.

To prove the above result we build on a technique that has been developed in the aforementioned prior works. The strategy is to first show the lower bound for a non-uniform subset distribution called a determinantal point process, where one can leverage additional properties to compute the expectation of a random projection. Then, one can show that a sufficiently large uniform sample contains a sample from the determinantal point process, which implies the desired lower bound.

Definition 3.3. *Given a PSD matrix $\mathbf{L} \in \mathcal{S}_m^+$, a determinantal point process $S \sim \text{DPP}(\mathbf{L})$ is a distribution over all sets $S \subseteq [m]$ such that $\Pr(S) \propto \det(\mathbf{L}_{S,S})$.*

Lemma 3.4 ([DM21]). *The expected size of $S \sim \text{DPP}(\mathbf{L})$ is $\mathbb{E}[|S|] = \text{tr}(\mathbf{L}(\mathbf{L} + \mathbf{I})^{-1})$.*

In our proof we will use the following black-box reduction from uniform sampling to a DPP, which first appeared in the proof of Lemma 4.3 in [DY24]. The version below is based on the proof of Lemma 10 in [DLNR24].

Lemma 3.5 ([DLNR24]). *Consider a PSD matrix $\mathbf{L} \in \mathcal{S}_m^+$, an $m \times m$ RHT matrix \mathbf{Q} , and $\delta > 0$ such that set $S_{\text{DPP}} \sim \text{DPP}(\mathbf{Q}\mathbf{L}\mathbf{Q}^\top)$ satisfies $k := \mathbb{E}[|S_{\text{DPP}}|] \geq C \log(m/\delta)$. Then, conditioned on an RHT property that holds with probability $1 - \delta$, a uniformly random set $S \sim \mathcal{U}(m, s)$ of size $s \geq Ck \log(k/\delta')$ can be coupled with S_{DPP} into a joint random variable (S, S_{DPP}) such that $S_{\text{DPP}} \subseteq S$ with probability $1 - \delta'$.*

To conclude the expected projection result from the above black-box reduction, [DLNR24] used a classical Cauchy-Binet-type determinantal summation formula (e.g., see Lemma 5 in [DKM20]), which shows that a DPP-sampled set $S_{\text{DPP}} \sim \text{DPP}(\frac{1}{\lambda}\mathbf{A}\mathbf{A}^\top)$ satisfies $\mathbb{E}[\mathbf{P}_{0,S_{\text{DPP}}}] = \mathbf{A}^\top(\mathbf{A}\mathbf{A}^\top + \bar{\lambda}\mathbf{I})^{-1}\mathbf{A}$, where $\mathbf{P}_{0,S_{\text{DPP}}} = \mathbf{A}_{S_{\text{DPP}}}^\top(\mathbf{A}_{S_{\text{DPP}}}\mathbf{A}_{S_{\text{DPP}}}^\top)^\dagger\mathbf{A}_{S_{\text{DPP}}}$ is the standard projection arising in block Kaczmarz. Then, one can convert from S_{DPP} to S by observing via Lemma 3.5 that $\mathbf{P}_{0,S} \succeq \mathbf{P}_{0,S_{\text{DPP}}}$ with probability $1 - \delta'$.

However, since we are bounding the expectation of a *regularized* projection matrix $\mathbf{P}_{\lambda,S}$, the classical Cauchy-Binet-type formula cannot be directly applied, and we no longer have a simple closed form expression for the expected regularized projection under DPP sampling. To address this, we show in Lemma 3.6 that if we sample according to a different DPP defined by matrix $\frac{m}{\lambda(m-k)}\bar{\mathbf{A}}\bar{\mathbf{A}}^\top + \frac{k}{m-k}\mathbf{I}$, then we can sufficiently bound the corresponding regularized projection by using the concept of “Regularized DPPs” originating from [DLM20] (for details see Appendix B). By combining the above discussion, we formally give the proof of Theorem 3.1.

Proof of Theorem 3.1. Let $\mathbf{A} = \mathbf{U}\Sigma\mathbf{V}^\top$ be its singular value decomposition and denote $\bar{\mathbf{U}} = \mathbf{Q}\mathbf{U}$. Define matrix $\mathbf{L} := \frac{m}{\lambda(m-k)}\mathbf{A}\mathbf{A}^\top + \frac{k}{m-k}\mathbf{I}$, and notice that¹

$$\begin{aligned} \mathbf{Q}\mathbf{L}\mathbf{Q}^\top &= \frac{m}{\lambda(m-k)}\bar{\mathbf{A}}\bar{\mathbf{A}}^\top + \frac{k}{m-k}\mathbf{I} \\ &= \bar{\mathbf{U}} \text{diag}\left(\frac{m\sigma_1^2}{\lambda(m-k)} + \frac{k}{m-k}, \dots, \frac{m\sigma_m^2}{\lambda(m-k)} + \frac{k}{m-k}\right)\bar{\mathbf{U}}^\top \end{aligned}$$

¹For convenience, in the case of $m > n$, we simply define $\sigma_{n+1} = \dots = \sigma_m = 0$.

is the eigendecomposition of matrix \mathbf{QLQ}^\top . By setting $\bar{\lambda} = \frac{1}{k} \sum_{i>k} \sigma_i^2$ and denoting $S_{\text{DPP}} \sim \text{DPP}(\frac{m}{\lambda(m-k)} \bar{\mathbf{A}} \bar{\mathbf{A}}^\top + \frac{k}{m-k} \mathbf{I})$, we can bound the expected sample size of S_{DPP} using Lemma 3.4 as follows:

$$\mathbb{E}[|S_{\text{DPP}}|] = \sum_{i=1}^m \frac{\frac{m}{\lambda(m-k)} \sigma_i^2 + \frac{k}{m-k}}{\frac{m}{\lambda(m-k)} \sigma_i^2 + \frac{k}{m-k} + 1} = \sum_{i=1}^m \frac{m \sigma_i^2 + \bar{\lambda} k}{m \sigma_i^2 + \bar{\lambda} m} = k + \sum_{i=1}^m \frac{(m-k) \sigma_i^2}{m \sigma_i^2 + \bar{\lambda} m} \geq k,$$

and a similar calculation shows $\mathbb{E}[|S_{\text{DPP}}|] \leq 3k$. Given $\delta, \delta' > 0$ and $k \geq C \log(m/\delta)$, let $S \sim \mathcal{U}(m, s)$ be a uniformly random set with $s \geq 3Ck \log(3k/\delta')$. By applying Lemma 3.5 to matrix \mathbf{L} , conditioned on an RHT property that holds with probability $1 - \delta$, we have $S_{\text{DPP}} \subseteq S$ holds with probability $1 - \delta'$. With the above analysis, we move on to the expectation of the ‘‘regularized’’ projection matrix. Using that $0 \leq \lambda \leq \frac{k}{m} \bar{\lambda}$, the following holds:

$$\begin{aligned} \mathbf{P}_{\lambda, S} &= \mathbf{A}_S^\top (\mathbf{A}_S \mathbf{A}_S^\top + \lambda \mathbf{I})^\dagger \mathbf{A}_S \\ &\succeq \mathbf{A}_S^\top \left(\mathbf{A}_S \mathbf{A}_S^\top + \frac{k \bar{\lambda}}{m} \mathbf{I} \right)^{-1} \mathbf{A}_S = \mathbf{I} - \frac{k \bar{\lambda}}{m} \cdot \left(\mathbf{A}_S^\top \mathbf{A}_S + \frac{k \bar{\lambda}}{m} \mathbf{I} \right)^{-1}. \end{aligned} \quad (3.1)$$

To bound the right hand side of (3.1) we use the following lemma, which bounds the corresponding term when sampling according to this specific DPP. The proof of Lemma 3.6 is based on the concept of Regularized DPP proposed by [DLM20], and we defer it to Appendix B.

Lemma 3.6. *Given $\mathbf{A} \in \mathbb{R}^{m \times n}$ and $k < \text{rank}(\mathbf{A})$, let $\bar{\lambda} = \frac{1}{k} \sum_{i>k} \sigma_i^2(\mathbf{A})$. Then, the random set $S_{\text{DPP}} \sim \text{DPP}(\frac{m}{\lambda(m-k)} \mathbf{A} \mathbf{A}^\top + \frac{k}{m-k} \mathbf{I})$ satisfies*

$$\mathbb{E} \left[\left(\mathbf{I} + \frac{m}{k \bar{\lambda}} \mathbf{A}_{S_{\text{DPP}}}^\top \mathbf{A}_{S_{\text{DPP}}} \right)^{-1} \right] \preceq \bar{\lambda} (\mathbf{A}^\top \mathbf{A} + \bar{\lambda} \mathbf{I})^{-1}. \quad (3.2)$$

Conditioned on the event $\mathcal{A}_0 := [S_{\text{DPP}} \subseteq S]$ (which holds with probability $1 - \delta'$), we have $\mathbf{A}_{S_{\text{DPP}}}^\top \mathbf{A}_{S_{\text{DPP}}} \preceq \mathbf{A}_S^\top \mathbf{A}_S$. Combining this with (3.1) and Lemma 3.6, we have the following holds:

$$\begin{aligned} \mathbb{E}[\mathbf{P}_{\lambda, S}] &= \mathbb{E}[\mathbf{P}_{\lambda, S} \mid \mathcal{A}_0] \Pr\{\mathcal{A}_0\} + \mathbb{E}[\mathbf{P}_{\lambda, S} \mid \mathcal{A}_0^c] \Pr\{\mathcal{A}_0^c\} \\ &\succeq \mathbb{E}[\mathbf{P}_{\lambda, S} \mid \mathcal{A}_0] \Pr\{\mathcal{A}_0\} \\ &\succeq \Pr\{\mathcal{A}_0\} \cdot \mathbf{I} - \frac{k \bar{\lambda}}{m} \cdot \mathbb{E} \left[\left(\mathbf{A}_S^\top \mathbf{A}_S + \frac{k \bar{\lambda}}{m} \mathbf{I} \right)^{-1} \mid \mathcal{A}_0 \right] \cdot \Pr\{\mathcal{A}_0\} \\ &\succeq \Pr\{\mathcal{A}_0\} \cdot \mathbf{I} - \mathbb{E} \left[\left(\frac{m}{k \bar{\lambda}} \mathbf{A}_{S_{\text{DPP}}}^\top \mathbf{A}_{S_{\text{DPP}}} + \mathbf{I} \right)^{-1} \mid \mathcal{A}_0 \right] \cdot \Pr\{\mathcal{A}_0\} \\ &\succeq (1 - \delta') \cdot \mathbf{I} - \bar{\lambda} (\mathbf{A}^\top \mathbf{A} + \bar{\lambda} \mathbf{I})^{-1} = \mathbf{A}^\top (\mathbf{A} \mathbf{A}^\top + \bar{\lambda} \mathbf{I})^{-1} \mathbf{A} - \delta' \mathbf{I}. \end{aligned}$$

Notice that the spectrum of matrix $\mathbf{A}^\top (\mathbf{A} \mathbf{A}^\top + \bar{\lambda} \mathbf{I})^{-1} \mathbf{A}$ can be expressed as $\{\frac{\sigma_i^2}{\sigma_i^2 + \bar{\lambda}}\}_i$, thus with the choice of $\bar{\lambda} = \frac{1}{k} \sum_{i>k} \sigma_i^2$ we have

$$\mathbf{A}^\top (\mathbf{A} \mathbf{A}^\top + \bar{\lambda} \mathbf{I})^{-1} \mathbf{A} \succeq \frac{(\sigma_{\min}^+)^2}{(\sigma_{\min}^+)^2 + \bar{\lambda}} \mathbf{I} = \frac{1}{1 + \frac{r-k}{k} \bar{\kappa}_k^2} \mathbf{I} \succeq \frac{k}{r \bar{\kappa}_k^2} \mathbf{I} \succeq \frac{k}{m \bar{\kappa}_k^2} \mathbf{I}.$$

By choosing $\delta' = \frac{k}{2r \bar{\kappa}_k^2}$ we have $\delta' \mathbf{I} \preceq \frac{1}{2} \mathbf{A}^\top (\mathbf{A} \mathbf{A}^\top + \bar{\lambda} \mathbf{I})^{-1} \mathbf{A}$, which gives $\mathbb{E}[\mathbf{P}_{\lambda, S}] \succeq \frac{1}{2} \mathbf{A}^\top (\mathbf{A} \mathbf{A}^\top + \bar{\lambda} \mathbf{I})^{-1} \mathbf{A}$, and the sample size needs to satisfy $s \geq O(k \log(k/\delta')) = O(k \log(r \bar{\kappa}_k))$. We also conclude that $\mu(\bar{\mathbf{A}}, \mathcal{U}(m, s), \lambda) = \lambda_{\min}^+(\mathbb{E}[\mathbf{P}_{\lambda, S}]) \geq \frac{k}{2r \bar{\kappa}_k^2}$. \square

3.2 Variance of the Regularized Projection

We now turn to bounding the term $\nu = \lambda_{\max}(\mathbb{E}[(\bar{\mathbf{P}}_\lambda^{\dagger/2} \mathbf{P}_{\lambda,S} \bar{\mathbf{P}}_\lambda^{\dagger/2})^2])$, where $\bar{\mathbf{P}}_\lambda = \mathbb{E}[\mathbf{P}_{\lambda,S}]$, which intuitively describes a notion of variance for the regularized projection $\mathbf{P}_{\lambda,S}$. This quantity was first introduced by [GHR18] in the case of $\lambda = 0$. They showed that $\frac{m}{s} \leq \nu \leq \frac{1}{\mu}$ for any matrix \mathbf{A} of rank m and random blocks S of size s , which unfortunately does not provide any acceleration guarantee. Recently, [DLNR24] gave an improved upper bound, but it came with trade-offs: Their bound, $\nu = \tilde{O}(\frac{m}{s} \bar{\kappa}_{k,l}^2)$, where $\bar{\kappa}_{k,l} := \frac{1}{l-k} \sum_{i=k+1}^l \sigma_i^2(\mathbf{A})$, requires replacing block sampling with a much more expensive sketching approach, due to their reliance on sophisticated tools from random matrix theory, and yet, it is still affected by a problem-dependent condition number $\bar{\kappa}_{k,l}$.

We use regularized projections to entirely avoid these trade-offs: Not only are we able to use block sampling (as opposed to expensive sketching), but also our proof is surprisingly elementary, and with the right choice of λ , we get a bound of $\nu = \tilde{O}(\frac{m}{s})$, without any problem-dependent condition number factors.

Theorem 3.7. *Given matrix $\mathbf{A} \in \mathbb{R}^{m \times n}$, parameters $\bar{\lambda} \geq \lambda > 0$, and a probability distribution \mathcal{D} over subsets of $[m]$, suppose that the corresponding regularized projection matrix $\mathbf{P}_{\lambda,S} := \mathbf{A}_S^\top (\mathbf{A}_S \mathbf{A}_S^\top + \lambda \mathbf{I})^{-1} \mathbf{A}_S$ satisfies:*

$$\bar{\mathbf{P}}_\lambda := \mathbb{E}_{S \sim \mathcal{D}}[\mathbf{P}_{\lambda,S}] \succeq c \mathbf{A}^\top (\mathbf{A}^\top \mathbf{A} + \bar{\lambda} \mathbf{I})^{-1},$$

for some $c > 0$. Then, it follows that:

$$\lambda_{\max} \left(\mathbb{E}[(\bar{\mathbf{P}}_\lambda^{\dagger/2} \mathbf{P}_{\lambda,S} \bar{\mathbf{P}}_\lambda^{\dagger/2})^2] \right) \leq \frac{2\bar{\lambda}}{c\lambda}.$$

Remark 3.8. *Under the assumptions of Theorem 3.1, applying Theorem 3.7 with $\lambda = \frac{k}{m} \bar{\lambda}$, we get $\nu(\bar{\mathbf{A}}, \mathcal{U}(m, s), \lambda) \leq \frac{4m}{k}$. Together with the bound on μ , this implies that $\bar{\rho}(\bar{\mathbf{A}}, \mathcal{U}(m, s), \lambda) \geq \frac{k}{3m\bar{\kappa}_k}$. Using Theorem 2.1, this obtains fast convergence for accelerated block Kaczmarz with fully random blocks. In the following section, we extend this analysis to capture block memoization, recovering Kaczmarz++.*

Proof of Theorem 3.7. By using the assumption we can bound the pseudoinverse of $\bar{\mathbf{P}}_\lambda = \mathbb{E}[\mathbf{P}_{\lambda,S}]$ as follows:

$$\bar{\mathbf{P}}_\lambda^\dagger \preceq \frac{1}{c} (\mathbf{A}^\top \mathbf{A} + \bar{\lambda} \mathbf{I}) (\mathbf{A}^\top \mathbf{A})^\dagger \preceq \frac{1}{c} (\mathbf{I} + \bar{\lambda} (\mathbf{A}^\top \mathbf{A})^\dagger), \quad (3.3)$$

which gives

$$\begin{aligned} \nu &= \left\| \mathbb{E}[\bar{\mathbf{P}}_\lambda^{\dagger/2} \mathbf{P}_{\lambda,S} \bar{\mathbf{P}}_\lambda^\dagger \mathbf{P}_{\lambda,S} \bar{\mathbf{P}}_\lambda^{\dagger/2}] \right\| = \left\| \bar{\mathbf{P}}_\lambda^{\dagger/2} \mathbb{E}[\mathbf{P}_{\lambda,S} \bar{\mathbf{P}}_\lambda^\dagger \mathbf{P}_{\lambda,S}] \bar{\mathbf{P}}_\lambda^{\dagger/2} \right\| \\ &\stackrel{(3.3)}{\leq} \frac{1}{c} \left\| \bar{\mathbf{P}}_\lambda^{\dagger/2} \mathbb{E}[\mathbf{P}_{\lambda,S}^2 + \bar{\lambda} \mathbf{P}_{\lambda,S} (\mathbf{A}^\top \mathbf{A})^\dagger \mathbf{P}_{\lambda,S}] \bar{\mathbf{P}}_\lambda^{\dagger/2} \right\| \\ &\leq \frac{1}{c} \left\| \bar{\mathbf{P}}_\lambda^{\dagger/2} \left(\mathbb{E}[\mathbf{P}_{\lambda,S}] + \bar{\lambda} \mathbb{E}[\mathbf{P}_{\lambda,S} (\mathbf{A}^\top \mathbf{A})^\dagger \mathbf{P}_{\lambda,S}] \right) \bar{\mathbf{P}}_\lambda^{\dagger/2} \right\| \\ &\leq \frac{1}{c} + \frac{\bar{\lambda}}{c} \left\| \bar{\mathbf{P}}_\lambda^{\dagger/2} \mathbb{E}[\mathbf{P}_{\lambda,S} (\mathbf{A}^\top \mathbf{A})^\dagger \mathbf{P}_{\lambda,S}] \bar{\mathbf{P}}_\lambda^{\dagger/2} \right\|. \end{aligned} \quad (3.4)$$

Notice that since $\lambda > 0$, we can express the middle term in (3.4) as follows:

$$\begin{aligned} \mathbf{P}_{\lambda,S} (\mathbf{A}^\top \mathbf{A})^\dagger \mathbf{P}_{\lambda,S} &= \mathbf{A}_S^\top (\mathbf{A}_S \mathbf{A}_S^\top + \lambda \mathbf{I})^{-1} \mathbf{I}_S \mathbf{A} (\mathbf{A}^\top \mathbf{A})^\dagger \mathbf{A}^\top \mathbf{I}_S^\top (\mathbf{A}_S \mathbf{A}_S^\top + \lambda \mathbf{I})^{-1} \mathbf{A}_S \\ &\preceq \mathbf{A}_S^\top (\mathbf{A}_S \mathbf{A}_S^\top + \lambda \mathbf{I})^{-1} \mathbf{I}_S \mathbf{I}_S^\top (\mathbf{A}_S \mathbf{A}_S^\top + \lambda \mathbf{I})^{-1} \mathbf{A}_S \\ &= \mathbf{A}_S^\top (\mathbf{A}_S \mathbf{A}_S^\top + \lambda \mathbf{I})^{-2} \mathbf{A}_S \end{aligned}$$

where the second step follows from the observation that $\mathbf{A}(\mathbf{A}^\top \mathbf{A})^\dagger \mathbf{A}^\top = \mathbf{A}\mathbf{A}^\dagger \preceq \mathbf{I}$, and the third step follows from $\mathbf{I}_S \mathbf{I}_S^\top = \mathbf{I}$. By taking expectation and using that $\mathbf{Z}\mathbf{X}\mathbf{Z}^\top \preceq \mathbf{Z}\mathbf{Y}\mathbf{Z}^\top$ holds whenever $\mathbf{X} \preceq \mathbf{Y}$, we have

$$\begin{aligned} \mathbb{E} \left[\mathbf{P}_{\lambda,S} (\mathbf{A}^\top \mathbf{A})^\dagger \mathbf{P}_{\lambda,S} \right] &\preceq \mathbb{E} \left[\mathbf{A}_S^\top (\mathbf{A}_S \mathbf{A}_S^\top + \lambda \mathbf{I})^{-2} \mathbf{A}_S \right] \\ &\preceq \frac{1}{\lambda} \mathbb{E} \left[\mathbf{A}_S^\top (\mathbf{A}_S \mathbf{A}_S^\top + \lambda \mathbf{I})^{-1} \mathbf{A}_S \right] = \frac{1}{\lambda} \mathbb{E} [\mathbf{P}_{\lambda,S}]. \end{aligned}$$

Finally by applying this result to (3.4) we have

$$\nu \leq \frac{1}{c} + \frac{\bar{\lambda}}{c\lambda} \left\| \bar{\mathbf{P}}_\lambda^{\dagger/2} \mathbb{E}[\mathbf{P}_{\lambda,S}] \bar{\mathbf{P}}_\lambda^{\dagger/2} \right\| \leq \frac{1}{c} + \frac{\bar{\lambda}}{c\lambda} \leq \frac{2\bar{\lambda}}{c\lambda}. \quad (3.5)$$

□

4 Optimized Computations via Block Memoization

The overall computational cost of Kaczmarz++ consists of the cost of applying the RHT plus the cost of performing its iterations. Next, in Section 4.1, we discuss the computational cost of computing the regularized projections, which dominate the overall computation in an iteration, but fortunately can be done inexactly. Then, in Section 4.2, we analyze our proposed block memoization, which reduces the number of Cholesky computations required for the regularized projections. Finally, we put everything together in Section 4.3, and summarize the overall computational costs in Theorem 4.5.

4.1 Computing the Projection Step

The dominant computational cost in each of the iterations is computing the regularized projection step \mathbf{w}_t , which can be formulated as standard under-determined least squares with Tikhonov regularization:

$$\mathbf{w}_t = \operatorname{argmin}_{\mathbf{w} \in \mathbb{R}^n} \left\{ \|\mathbf{A}_S \mathbf{w} - \mathbf{r}_t\|^2 + \lambda \|\mathbf{w}\|^2 \right\}, \quad \text{where } \mathbf{r}_t = \mathbf{A}_S \mathbf{x}_t - \mathbf{b}_S.$$

This step can be computed directly using $O(ns^2)$ arithmetic operations for a block of size s , which may be acceptable for small s , but becomes prohibitive for large block sizes. However, since our convergence analysis allows computing \mathbf{w}_t inexactly, we can also use a preconditioned iterative solver such as CG or LSQR. Here, we propose a randomized preconditioning strategy based on sketching, where one constructs a small sketch $\hat{\mathbf{A}} = \mathbf{A}_S \mathbf{\Pi}^\top \in \mathbb{R}^{s \times \tau}$ for a sketching matrix $\mathbf{\Pi} \in \mathbb{R}^{\tau \times n}$, and then use this sketch to construct a preconditioner. Given the extensive literature on randomized sketching (e.g., see [DM16, MT20, DM24]), there are several different preconditioner constructions one can use, such as Blendenpik [AMT10] and LSRN [MSM14]. Of particular relevance here are approaches that exploit the presence of regularization λ to improve the quality of the preconditioner. Here, we will describe the Cholesky-based preconditioner of [MN22], due to its simplicity and numerical stability:

- 1: Compute $\hat{\mathbf{A}} = \mathbf{A}_S \mathbf{\Pi}^\top$, where $\mathbf{\Pi} \in \mathbb{R}^{\tau \times s}$ is a random sketching matrix;
- 2: Compute $\mathbf{R} = \operatorname{chol}(\hat{\mathbf{A}} \hat{\mathbf{A}}^\top + \lambda \mathbf{I})$, where $\operatorname{chol}()$ is the Cholesky factorization.

Armed with this Cholesky preconditioner \mathbf{R} , we can now compute \mathbf{w}_t as part of the min-length solution to the following system using an iterative method such as LSQR:

$$\begin{bmatrix} \mathbf{w}_t \\ \mathbf{v}_t \end{bmatrix} = \underset{\mathbf{w} \in \mathbb{R}^n, \mathbf{v} \in \mathbb{R}^s}{\operatorname{argmin}} \left\| \mathbf{R}^{-\top} [\mathbf{A}_S \sqrt{\lambda} \mathbf{I}] \begin{bmatrix} \mathbf{w} \\ \mathbf{v} \end{bmatrix} - \mathbf{R}^{-\top} \mathbf{r}_t \right\|^2. \quad (4.1)$$

The quality of the preconditioning is determined primarily by the choice of sketch size τ . In particular, to ensure that the system (4.1) has condition number $O(1)$, it suffices to use sketch size τ proportional to the so-called λ -effective dimension $d_\lambda(\mathbf{A}_S) = \sum_{i=1}^s \frac{\sigma_i^2(\mathbf{A}_S)}{\sigma_i^2(\mathbf{A}_S) + \lambda}$. Note that $d_\lambda(\mathbf{A}_S) \leq s$ for any $\lambda \geq 0$, and moreover, larger λ yields smaller $d_\lambda(\mathbf{A}_S)$, which means that introducing regularization makes it easier to precondition the projection step. We illustrate this in the case when $\mathbf{\Pi}$ is the Subsampled Randomized Hadamard Transform (SRHT, [AC09, Tro11]), although similar guarantees can be obtained, e.g., for sparse sketching matrices [CW13, CDDR24].

Lemma 4.1. *For $\mathbf{A}_S \in \mathbb{R}^{s \times n}$ and $\lambda \geq 0$, if $\mathbf{\Pi} = \sqrt{\frac{n}{\tau}} \mathbf{I}_T \mathbf{Q}$ where \mathbf{Q} is the RHT and T is a uniformly random set of size $\tau \geq C(d_\lambda(\mathbf{A}_S) + \log(n/\delta)) \log(d_\lambda(\mathbf{A}_S)/\delta)$, then with probability $1 - \delta$ we have $\kappa(\mathbf{R}^{-\top} [\mathbf{A}_S \sqrt{\lambda} \mathbf{I}]) \leq 2$, and after $O(\log(\kappa_S/\epsilon))$ iterations of LSQR on (4.1), we get $\tilde{\mathbf{w}}$ such that $\|\tilde{\mathbf{w}} - \mathbf{w}_t\| \leq \epsilon \|\mathbf{w}_t\|$, where $\kappa_S = \max\{1, \sqrt{\lambda}/\sigma_{\min}(\mathbf{A}_S)\}$.*

Proof. The bound $\kappa(\mathbf{R}^{-\top} [\mathbf{A}_S \sqrt{\lambda} \mathbf{I}]) \leq 2$ follows from standard analysis of sketching, e.g., see Theorem 3.5 in [MN22] and the associated discussion. LSQR initialized with zeros after $O(\log 1/\epsilon)$ iterations returns vectors $\tilde{\mathbf{w}}$ and $\tilde{\mathbf{v}}$ such that:

$$\left\| \begin{bmatrix} \tilde{\mathbf{w}} \\ \tilde{\mathbf{v}} \end{bmatrix} - \begin{bmatrix} \mathbf{w}_t \\ \mathbf{v}_t \end{bmatrix} \right\| \leq \epsilon \sqrt{\kappa(\mathbf{M})} \cdot \left\| \begin{bmatrix} \mathbf{w}_t \\ \mathbf{v}_t \end{bmatrix} \right\|, \quad \text{for } \mathbf{M} = \begin{bmatrix} \mathbf{A}_S^\top \\ \sqrt{\lambda} \mathbf{I} \end{bmatrix} \mathbf{R}^{-1} \mathbf{R}^{-\top} [\mathbf{A}_S \sqrt{\lambda} \mathbf{I}].$$

From the condition number bound we have that $\kappa(\mathbf{M}) \leq 4$, so we can now recover the error bound for $\tilde{\mathbf{w}}$ as follows:

$$\|\tilde{\mathbf{w}} - \mathbf{w}_t\| \leq \sqrt{\|\tilde{\mathbf{w}} - \mathbf{w}_t\|^2 + \|\tilde{\mathbf{v}} - \mathbf{v}_t\|^2} \leq 2\epsilon \sqrt{\|\mathbf{w}_t\|^2 + \|\mathbf{v}_t\|^2}.$$

Since $\mathbf{w}_t = \mathbf{A}_S^\top (\mathbf{A}_S \mathbf{A}_S^\top + \lambda \mathbf{I})^{-1} \mathbf{r}_t$ and $\mathbf{v}_t = \sqrt{\lambda} (\mathbf{A}_S \mathbf{A}_S^\top + \lambda \mathbf{I})^{-1} \mathbf{r}_t$, it follows that $\mathbf{w}_t = \frac{1}{\sqrt{\lambda}} \mathbf{A}_S^\top \mathbf{v}_t$. This implies that $\|\mathbf{v}_t\| \leq \kappa_S \|\mathbf{w}_t\|$, and so $\|\tilde{\mathbf{w}} - \mathbf{w}_t\| \leq 2\epsilon(1 + \kappa_S) \|\mathbf{w}_t\|$. Adjusting ϵ appropriately concludes the proof. \square

Constructing the preconditioner \mathbf{R} takes $O(T_{\text{sketch}} + \tau s^2 + s^3)$ operations, where T_{sketch} represents the cost of the matrix product $\mathbf{A}_S \mathbf{\Pi}^\top$. For example, when $\mathbf{\Pi}$ is the SRHT, as in Lemma 4.1, then $T_{\text{sketch}} = O(ns \log n)$. Thus, setting $\tau = O(s \log s)$, the overall cost of solving the projection step to within ϵ relative accuracy takes no more than $O(ns \log n + s^3 \log s)$ operations for constructing \mathbf{R} , followed by $O(ns \log(\kappa_S/\epsilon))$ operations for running LSQR.

We note that more elaborate randomized preconditioning schemes exist for regularized least squares, such as the SVD-based preconditioner of [MN22], and the KRR-based preconditioners of [ACW17, FTU23], which can be computed with $O(T_{\text{sketch}} + \tau^2 s)$ operations. These approaches may be preferable when using $\tau \ll s$. However, given that the matrix \mathbf{A}_S is itself random, it may be difficult to find the optimal value of τ in each step, which is why we recommend the simple choice of $\tau = \tilde{O}(s)$.

4.2 Block Memoization

When the block size s is larger than $O(\sqrt{n})$, then the $O(s^3)$ cost of computing the Cholesky factor \mathbf{R} dominates the remaining $\tilde{O}(ns)$ operations required for performing the projection step. This raises the question of whether we can reuse the \mathbf{R} computed in one step for any future steps. Naturally, we could do that if we encounter the same block set S again in a subsequent iteration, but when sampling among all $\binom{m}{s}$ sets, this is very unlikely. To address this, we propose sampling among a small collection of blocks, $\mathcal{B} \subseteq \binom{[m]}{s}$. That way, we only have to compute $|\mathcal{B}|$ Cholesky factors, which can then be reused to speed up later iterations of the algorithm. This strategy, which we call *block memoization*, enables using Kaczmarz++ effectively with even larger block sizes.

The crucial challenge with *block memoization* is to ensure that the reduced amount of randomness in the block sampling scheme does not adversely affect the convergence rate. This challenge has been encountered by prior works which have considered sampling from a small collection of blocks, including the classical variant of block Kaczmarz [Elf80] where the rows of \mathbf{A} are partitioned into m/s blocks of size s . However, despite efforts [NT14], sharp convergence analysis for a partition-based block Kaczmarz has proven elusive.

We demonstrate that, once again, introducing regularized projections resolves this crucial challenge: We show that Algorithm 1 using a collection \mathcal{B} consisting of $O(\frac{m}{k} \log n)$ uniformly random blocks of size $s = \tilde{O}(k)$ achieves nearly the same (up to factor 2) convergence rate as if it was sampling from all $\binom{[m]}{s}$ blocks. Importantly, this is more blocks than the m/s that would be obtained by simply partitioning the rows, but only by a logarithmic factor. This over-sampling factor appears necessary for fast convergence even in practice.

Theorem 4.2 (Block memoization). *Consider matrix $\mathbf{A} \in \mathbb{R}^{m \times n}$, parameters $\bar{\lambda} \geq \lambda > 0$, and a probability distribution \mathcal{D} over subsets of $[m]$, such that the regularized projection matrix $\mathbf{P}_{\lambda,S} := \mathbf{A}_S^\top (\mathbf{A}_S \mathbf{A}_S^\top + \lambda \mathbf{I})^{-1} \mathbf{A}_S$ satisfies:*

$$\bar{\mathbf{P}}_\lambda := \mathbb{E}_{S \sim \mathcal{D}}[\mathbf{P}_{\lambda,S}] \succeq c \mathbf{A}^\top \mathbf{A} (\mathbf{A}^\top \mathbf{A} + \bar{\lambda} \mathbf{I})^{-1}$$

for some $c > 0$. Let $\mathcal{B} = \{S_i\}_{i=1}^B$ be a collection of B independent samples from \mathcal{D} . If $B \geq \frac{4(7c+13)\bar{\lambda}}{3c\lambda} \log(2n/\delta)$, then with probability $1 - \delta$, the collection \mathcal{B} satisfies:

$$\frac{1}{B} \sum_{j=1}^B \mathbf{P}_{\lambda,S_j} \succeq \frac{1}{2} \bar{\mathbf{P}}_\lambda.$$

To prove Theorem 4.2, we rely on the following Bernstein's inequality for the concentration of symmetric random matrices, adapted from [Tro15].

Lemma 4.3 (Matrix Bernstein). *Let $\mathbf{Z}_1, \dots, \mathbf{Z}_B$ be independent random symmetric $n \times n$ matrices such that $\frac{1}{B} \sum_j \mathbb{E}[\mathbf{Z}_j] = \bar{\mathbf{Z}}$ and $\|\frac{1}{B} \sum_j \mathbb{E}[(\mathbf{Z}_j - \bar{\mathbf{Z}})^2]\| \leq \sigma^2$. Suppose we have $\|\mathbf{Z}_j - \mathbb{E}[\mathbf{Z}_j]\| \leq R$ holds for all $j \in [B]$. Then for any $\epsilon \geq 0$,*

$$\Pr \left(\left\| \frac{1}{B} \sum_{j=1}^B \mathbf{Z}_j - \bar{\mathbf{Z}} \right\| \geq \epsilon \right) \leq 2n \cdot \exp \left(- \frac{\epsilon^2 B/2}{\sigma^2 + \epsilon R/3} \right).$$

Proof of Theorem 4.2. Let $\mathbf{Z}_j := \bar{\mathbf{P}}_\lambda^{\dagger/2} \mathbf{P}_{\lambda,S_j} \bar{\mathbf{P}}_\lambda^{\dagger/2}$ be a normalized form of the regularized projection matrix \mathbf{P}_{λ,S_j} associated with subset S_j from \mathcal{B} . Then, we have $\mathbb{E}_{S_j \sim \mathcal{D}}[\mathbf{Z}_j] = \bar{\mathbf{P}}_\lambda^{\dagger/2} \bar{\mathbf{P}}_\lambda \bar{\mathbf{P}}_\lambda^{\dagger/2}$. In order

to apply matrix Bernstein and give a concentration result, we will bound $\|\mathbf{Z}_j - \bar{\mathbf{P}}_\lambda^{\dagger/2} \bar{\mathbf{P}}_\lambda \bar{\mathbf{P}}_\lambda^{\dagger/2}\|$ and $\|\mathbb{E}_{S_j \sim \mathcal{D}}[(\mathbf{Z}_j - \bar{\mathbf{P}}_\lambda^{\dagger/2} \bar{\mathbf{P}}_\lambda \bar{\mathbf{P}}_\lambda^{\dagger/2})^2]\|$. For the second term, we have

$$\begin{aligned} \|\mathbb{E}_{S_j \sim \mathcal{D}}[(\mathbf{Z}_j - \bar{\mathbf{P}}_\lambda^{\dagger/2} \bar{\mathbf{P}}_\lambda \bar{\mathbf{P}}_\lambda^{\dagger/2})^2]\| &= \|\bar{\mathbf{P}}_\lambda^{\dagger/2} \mathbb{E}[(\mathbf{P}_{\lambda, S_j} - \bar{\mathbf{P}}_\lambda) \bar{\mathbf{P}}_\lambda^\dagger (\mathbf{P}_{\lambda, S_j} - \bar{\mathbf{P}}_\lambda)] \bar{\mathbf{P}}_\lambda^{\dagger/2}\| \\ &= \|\bar{\mathbf{P}}_\lambda^{\dagger/2} (\mathbb{E}[\mathbf{P}_{\lambda, S_j} \bar{\mathbf{P}}_\lambda^\dagger \mathbf{P}_{\lambda, S_j}] - \bar{\mathbf{P}}_\lambda \bar{\mathbf{P}}_\lambda^\dagger \bar{\mathbf{P}}_\lambda) \bar{\mathbf{P}}_\lambda^{\dagger/2}\| \\ &= \|\mathbb{E}[\bar{\mathbf{P}}_\lambda^{\dagger/2} \mathbf{P}_{\lambda, S_j} \bar{\mathbf{P}}_\lambda^\dagger \mathbf{P}_{\lambda, S_j} \bar{\mathbf{P}}_\lambda^{\dagger/2}] - \bar{\mathbf{P}}_\lambda^{\dagger/2} \bar{\mathbf{P}}_\lambda \bar{\mathbf{P}}_\lambda^{\dagger/2}\| \\ &\leq \|\mathbb{E}[(\bar{\mathbf{P}}_\lambda^{\dagger/2} \mathbf{P}_{\lambda, S_j} \bar{\mathbf{P}}_\lambda^{\dagger/2})^2]\| + 1 = \nu + 1, \end{aligned}$$

where the last step follows from the definition of $\nu = \nu(\mathbf{A}, \mathcal{D}, \lambda)$ in (2.1). According to Theorem 3.7, under the same assumption we have $\nu \leq \frac{2\bar{\lambda}}{c\lambda}$. By applying this result we obtain the bound $\|\mathbb{E}_{S_j \sim \mathcal{D}}[(\mathbf{Z}_j - \bar{\mathbf{P}}_\lambda^{\dagger/2} \bar{\mathbf{P}}_\lambda \bar{\mathbf{P}}_\lambda^{\dagger/2})^2]\| \leq \frac{2\bar{\lambda}}{c\lambda} + 1 =: \sigma^2$.

Next, to obtain the R term in Bernstein's inequality, notice that according to our assumption, $\bar{\mathbf{P}}_\lambda^\dagger \preceq \frac{1}{c}(\mathbf{A}^\top \mathbf{A} + \bar{\lambda} \mathbf{I})(\mathbf{A}^\top \mathbf{A})^\dagger =: \boldsymbol{\Sigma}$, thus we have

$$\|\mathbf{Z}_j\| \leq \|\boldsymbol{\Sigma}^{1/2} \mathbf{P}_{\lambda, S_j} \boldsymbol{\Sigma}^{1/2}\| = \|\boldsymbol{\Sigma}^{1/2} \mathbf{A}^\top \mathbf{I}_S^\top (\mathbf{A}_S \mathbf{A}_S^\top + \lambda \mathbf{I})^{-1} \mathbf{I}_S \mathbf{A} \boldsymbol{\Sigma}^{1/2}\|.$$

Letting $\mathbf{A} = \mathbf{U} \mathbf{D} \mathbf{V}^\top$ be the compact SVD of \mathbf{A} , note that $\boldsymbol{\Sigma} \mathbf{A}^\top = \frac{1}{c} \mathbf{V} (\mathbf{D}^2 + \bar{\lambda} \mathbf{I})^{1/2} \mathbf{U}^\top$. So, additionally observing that $\mathbf{U} (\mathbf{D}^2 + \bar{\lambda} \mathbf{I}) \mathbf{U}^\top \preceq \mathbf{A} \mathbf{A}^\top + \bar{\lambda} \mathbf{I} \preceq \frac{\bar{\lambda}}{\lambda} (\mathbf{A} \mathbf{A}^\top + \lambda \mathbf{I})$, we get

$$\begin{aligned} \|\mathbf{Z}_j\| &\leq \frac{1}{c} \|\mathbf{V} (\mathbf{D}^2 + \bar{\lambda} \mathbf{I})^{1/2} \mathbf{U}^\top \mathbf{I}_S^\top (\mathbf{A}_S \mathbf{A}_S^\top + \lambda \mathbf{I})^{-1} \mathbf{I}_S \mathbf{U} (\mathbf{D}^2 + \bar{\lambda} \mathbf{I})^{1/2} \mathbf{V}^\top\| \\ &= \frac{1}{c} \|(\mathbf{A}_S \mathbf{A}_S^\top + \lambda \mathbf{I})^{-1/2} \mathbf{I}_S \mathbf{U} (\mathbf{D}^2 + \bar{\lambda} \mathbf{I}) \mathbf{U}^\top \mathbf{I}_S^\top (\mathbf{A}_S \mathbf{A}_S^\top + \lambda \mathbf{I})^{-1/2}\| \\ &\leq \frac{\bar{\lambda}}{c\lambda} \|(\mathbf{A}_S \mathbf{A}_S^\top + \lambda \mathbf{I})^{-1/2} \mathbf{I}_S (\mathbf{A} \mathbf{A}^\top + \lambda \mathbf{I}) \mathbf{I}_S^\top (\mathbf{A}_S \mathbf{A}_S^\top + \lambda \mathbf{I})^{-1/2}\| = \frac{\bar{\lambda}}{c\lambda}. \end{aligned}$$

This gives us the R term in Bernstein's inequality:

$$\|\mathbf{Z}_j - \bar{\mathbf{P}}_\lambda^{\dagger/2} \bar{\mathbf{P}}_\lambda \bar{\mathbf{P}}_\lambda^{\dagger/2}\| \leq \|\mathbf{Z}_j\| + \|\bar{\mathbf{P}}_\lambda^{\dagger/2} \bar{\mathbf{P}}_\lambda \bar{\mathbf{P}}_\lambda^{\dagger/2}\| \leq \frac{\bar{\lambda}}{c\lambda} + 1 \leq \frac{(c+1)\bar{\lambda}}{c\lambda} =: R.$$

Applying Lemma 4.3 to matrices $\{\mathbf{Z}_j\}_{j=1}^B$ with parameters $R = \frac{(c+1)\bar{\lambda}}{c\lambda}$ and $\sigma^2 = \frac{2\bar{\lambda}}{c\lambda} + 1$, we conclude that if we set $B \geq \frac{4(7c+13)\bar{\lambda}}{3c\lambda} \log(2n/\delta)$ and $\bar{\mathbf{Z}} = \bar{\mathbf{P}}_\lambda^{\dagger/2} \bar{\mathbf{P}}_\lambda \bar{\mathbf{P}}_\lambda^{\dagger/2}$, then

$$\Pr \left(\left\| \frac{1}{B} \sum_{j=1}^B \mathbf{Z}_j - \bar{\mathbf{Z}} \right\| \geq \frac{1}{2} \right) \leq 2n \cdot \exp \left(-\frac{B/8}{\frac{2\bar{\lambda}}{c\lambda} + 1 + \frac{(c+1)\bar{\lambda}}{6c\lambda}} \right) \leq \delta.$$

So, the average $\hat{\mathbf{Z}} := \frac{1}{B} \sum_{j=1}^B \mathbf{Z}_j$ satisfies $\hat{\mathbf{Z}} \succeq \bar{\mathbf{Z}} - \frac{1}{2} \mathbf{I}$ with probability $1 - \delta$. Note that $\bar{\mathbf{Z}}$ is a projection onto a subspace that contains the range of $\hat{\mathbf{Z}}$, so applying $\bar{\mathbf{Z}}$ on both sides of that inequality we get $\hat{\mathbf{Z}} = \bar{\mathbf{Z}} \hat{\mathbf{Z}} \bar{\mathbf{Z}} \succeq \bar{\mathbf{Z}} \bar{\mathbf{Z}} \bar{\mathbf{Z}} - \frac{1}{2} \bar{\mathbf{Z}} \bar{\mathbf{Z}} = \frac{1}{2} \bar{\mathbf{Z}}$. This gives

$$\frac{1}{B} \sum_{j=1}^B \mathbf{P}_{\lambda, S_j} \succeq \bar{\mathbf{P}}_\lambda^{1/2} \hat{\mathbf{Z}} \bar{\mathbf{P}}_\lambda^{1/2} \succeq \frac{1}{2} \bar{\mathbf{P}}_\lambda^{1/2} \bar{\mathbf{Z}} \bar{\mathbf{P}}_\lambda^{1/2} = \frac{1}{2} \bar{\mathbf{P}}_\lambda.$$

□

Combining Theorem 4.2 with the analysis of μ and ν in Theorems 3.1 and 3.7, as well as the acceleration analysis from Theorem 2.1, we can now recover the convergence guarantee for Kaczmarz++ (Algorithm 1).

Corollary 4.4. *Suppose $\mathbf{A} \in \mathbb{R}^{m \times n}$ is transformed by RHT, i.e., $\bar{\mathbf{A}} = \mathbf{Q}\mathbf{A}$. Let $\sigma_1 \geq \sigma_2 \geq \dots$ be \mathbf{A} 's singular values. Given $\delta \in (0, 1)$ and $C \log(m/\delta) \leq k < \text{rank}(\mathbf{A})$, let $\lambda = \frac{1}{m} \sum_{i>k} \sigma_i^2$. If \mathcal{B} consists of $O(\frac{m}{k} \log(n/\delta))$ uniformly random sets from $\binom{[m]}{s}$ for $s \geq Ck \log(m\bar{\kappa}_k)$ and $\mathcal{U}(\mathcal{B})$ is the uniform distribution over \mathcal{B} , then with prob. $1 - \delta$:*

$$\mu(\bar{\mathbf{A}}, \mathcal{U}(\mathcal{B}), \lambda) \geq \frac{k}{4m\bar{\kappa}_k^2}, \quad \nu(\bar{\mathbf{A}}, \mathcal{U}(\mathcal{B}), \lambda) \leq \frac{8m}{k} \quad \text{and} \quad \bar{\rho}(\bar{\mathbf{A}}, \mathcal{U}(\mathcal{B}), \lambda) \geq \frac{k}{6m\bar{\kappa}_k}.$$

Thus, via Theorem 2.1, Kaczmarz++ with $\rho = \bar{\rho}/2$ and $\eta = \frac{1}{2\nu}$ satisfies:

$$\mathbb{E} \|\mathbf{x}_t - \mathbf{x}^*\|^2 \leq 8 \left(1 - \frac{k}{24m\bar{\kappa}_k}\right)^t \|\mathbf{x}_0 - \mathbf{x}^*\|^2.$$

4.3 Overall Computational Analysis

In this section, we illustrate how all of the above results can be put together to achieve low computational cost for Kaczmarz++. For clarity, we make a few simplifying assumptions: we let \mathbf{A} have full row rank (although similar claims can be recovered for any consistent linear system), and we allow optimal selection of the algorithmic hyper-parameters. Note that all of our intermediate results show that the algorithm is robust to different choices of parameters λ , ρ , η , and B , and in the following section, we discuss how to select these parameters in practice.

Theorem 4.5 (Computational analysis). *Given matrix $\mathbf{A} \in \mathbb{R}^{m \times n}$ with rank $m \leq n$, and $\mathbf{b} \in \mathbb{R}^n$, let \mathbf{x}^* be the minimum-norm solution of $\mathbf{A}\mathbf{x} = \mathbf{b}$. For $\delta \in (0, 1)$ and $C \log(m/\delta) \leq k < m$, Kaczmarz++ (Alg. 1) with block size $s = \lceil Ck \log(m\bar{\kappa}_k) \rceil$, $\lambda = \frac{1}{m} \sum_{i>k} \sigma_i^2(\mathbf{A})$, $\rho = \frac{k}{12m\bar{\kappa}_k}$, $\eta = \frac{k}{16m}$, $\mathbf{x}_0 = \mathbf{0}_n$, and $B = \lceil C\frac{m}{k} \log(m/\delta) \rceil$, after $t = O(\frac{m}{k} \bar{\kappa}_k \log 1/\epsilon\delta)$ iterations, with probability $1 - \delta$ satisfies*

$$\|\mathbf{x}_t - \mathbf{x}^*\| \leq \epsilon \|\mathbf{x}^*\| \quad \text{using} \quad \tilde{O}(mk^2 + mn\bar{\kappa}_k \log 1/\epsilon\delta) \quad \text{operations.}$$

Remark 4.6. *Similar guarantee (up to logarithmic factors) can be recovered for Kaczmarz++ running on a consistent over-determined linear system (i.e., $m \geq n$).*

Proof. Corollary 4.4 implies that it takes $t = O(\frac{m}{k} \bar{\kappa}_k \log 1/\epsilon)$ iterations to converge ϵ -close in expectation. We convert this to a guarantee that holds with $1 - \delta$ probability by replacing ϵ with $\epsilon\delta$ and then applying Markov's inequality.

It remains to bound the costs associated with running the algorithm.

1. First, applying the RHT takes $O(mn \log m)$ operations.
2. Then, computing all of the Cholesky factors takes $O(B(ns \log n + s^3 \log s)) = O(mn \log^3(m\bar{\kappa}_k/\delta) + mk^2 \log k \log^4(m\bar{\kappa}_k))$.
3. Finally, each iteration of the algorithm requires solving (4.1) with LSQR so that $\|\tilde{\mathbf{w}}_t - \mathbf{w}_t\| \leq \epsilon \|\mathbf{w}_t\|$ for $\epsilon \leq \frac{k}{Cm\bar{\kappa}_k^2}$, which for a given block S takes $O(ns \log(\kappa_S/\epsilon))$, where $\kappa_S = \sqrt{\lambda}/\sigma_{\min}(\mathbf{A}_S)$. Note that since \mathbf{A} has full row rank, $\sigma_{\min}(\mathbf{A}_S) \geq \sigma_{\min}(\mathbf{A})$, so thanks to our choice of λ , we have $\kappa_S \leq \bar{\kappa}_k$ for any S . Thus, the cost of each iteration is $O(nk \log^2(n\bar{\kappa}_k))$. Multiplying by t , we get $O(mn\bar{\kappa}_k \log^2(n\bar{\kappa}_k) \log(1/\epsilon\delta))$ operations.

Adding all of these costs together, we recover the claim. \square

5 Improved Algorithm for Positive Semidefinite Systems

In this section, we propose a specialized implementation of Kaczmarz++ as a coordinate descent-type solver (CD++, Algorithm 3), which is optimized for square positive semidefinite linear systems. This algorithm not only gets an improved convergence rate compared to Kaczmarz++ for PSD matrices, but also admits a simplified block memoization scheme that avoids an inner LSQR solver. Along the way, we describe a novel adaptive scheme for tuning the acceleration parameters (relevant for both Kaczmarz++ and CD++), as well as a fast implementation of the randomized Hadamard transform for symmetric matrices.

5.1 Coordinate Descent

When the matrix \mathbf{A} is PSD, then Kaczmarz++ admits a specialized formulation as a block coordinate descent method, similarly as can be done for the classical randomized Kaczmarz algorithm, see e.g. [HNR17, Pet15]. To see this, let $\tilde{\mathbf{x}} = \mathcal{A}(\mathbf{A}, \mathbf{b}, \mathbf{x}_0)$ denote the output of Algorithm 1 for solving a general linear system $\mathbf{A}\mathbf{x} = \mathbf{b}$ (for now, skipping the RHT step), initialized with \mathbf{x}_0 . Now, if we are given an $n \times n$ PSD matrix, $\mathbf{A} \in \mathcal{S}_n^+$, then we can write $\mathbf{A} = \Phi\Phi^\top$ for some Φ (for example, the square root of \mathbf{A}), and so we can rewrite $\mathbf{A}\mathbf{x} = \mathbf{b}$ as:

$$\Phi\mathbf{z} = \mathbf{b} \quad \text{for } \mathbf{z} = \Phi^\top\mathbf{x}.$$

Thus, instead of solving the system $\mathbf{A}\mathbf{x} = \mathbf{b}$ directly, we consider implicitly applying our block Kaczmarz algorithm to $\Phi\mathbf{z} = \mathbf{b}$, i.e., computing $\Phi^\top\tilde{\mathbf{x}} = \mathcal{A}(\Phi, \mathbf{b}, \Phi^\top\mathbf{x}_0)$. For this procedure, letting $\mathbf{z}_t = \Phi^\top\mathbf{x}_t$ be the implicit Kaczmarz++ iterates, we get:

$$\mathbf{w}_t = \Phi_S^\top(\Phi_S\Phi_S^\top + \lambda\mathbf{I})^{-1}(\Phi_S\mathbf{z}_t - \mathbf{b}_S) = \Phi^\top\mathbf{I}_S^\top(\mathbf{A}_{S,S} + \lambda\mathbf{I})^{-1}(\mathbf{A}_S\mathbf{x}_t - \mathbf{b}_S). \quad (5.1)$$

This leads to the following coordinate descent update (line 11 in Algorithm 3):

$$\mathbf{w}_t^{\text{cd}} = \mathbf{I}_S^\top(\mathbf{A}_{S,S} + \lambda\mathbf{I})^{-1}(\mathbf{A}_S\mathbf{x}_t - \mathbf{b}_S).$$

Thus, the convergence rate of CD++ is determined by the convergence of the implicit Kaczmarz++ algorithm, since $\|\mathbf{z}_t - \mathbf{z}^*\| = \|\Phi^\top(\mathbf{x}_t - \mathbf{x}^*)\| = \|\mathbf{x}_t - \mathbf{x}^*\|_{\mathbf{A}}$. Crucially, this convergence is now governed by $\bar{\kappa}_k(\Phi) \leq \bar{\kappa}_k(\mathbf{A})$, hence the improvement over simply running Kaczmarz++ on \mathbf{A} .

5.2 Simplified Block Memoization

One of the main costs in the above block coordinate descent update is applying the inverse matrix $(\mathbf{A}_{S,S} + \lambda\mathbf{I})^{-1}$ to a vector. Similarly to what we did in Section 4, we can amortize this cost by sampling a collection of blocks, and pre-computing the Cholesky factors of $\mathbf{A}_{S,S} + \lambda\mathbf{I}$, so that all subsequent applications of $(\mathbf{A}_{S,S} + \lambda\mathbf{I})^{-1}$ can be done using $O(s^2)$ operations, where s is the block size. Note that, there is no need for sketching or using LSQR in the CD++ version of this scheme, because we can compute the Cholesky factor exactly in $O(s^3)$ time, unlike in Kaczmarz++, where this would take $O(ns^2)$ time (Section 4.1).

The key question is how to choose the number of blocks to pre-compute, in order to ensure effective convergence of the method. Our theory suggests that $O(\frac{n}{k} \log n)$ blocks is enough with high probability when block size is $s = \tilde{O}(k)$, but the constant/logarithmic factors matter significantly, since if we choose too few blocks up front, we may not end up with a convergent method, whereas too many blocks leads to significant unnecessary computational overhead. To address this, we propose an online block selection scheme, where the algorithm adds new blocks during the course of its convergence, but gradually shifts towards reusing the previously collected blocks.

Specifically, we initialize our block list \mathcal{B} as empty, and then in iteration t :

1. Sample a Bernoulli variable b with success probability $\min\{1, \frac{1}{t} \cdot \frac{n}{s} \log n\}$.
2. If $b = 1$, then sample new random block S from $\binom{[n]}{s}$, store the Cholesky factor $\mathbf{R}[S] = \text{chol}(\mathbf{A}_{S,S} + \lambda \mathbf{I}) \in \mathbb{R}^{s \times s}$, and add S to the list \mathcal{B} .
3. If $b = 0$, then sample block S from \mathcal{B} , and reuse the saved Cholesky $\mathbf{R}[S]$.

This block selection strategy implies that the first $B = \frac{n}{s} \log n$ blocks will be sampled uniformly at random from all size s index sets and added to the block list \mathcal{B} . After that, in T iterations the scheme will collect on average an additional $\sum_{t=B}^T \frac{B}{t} \approx B \log(\frac{T}{B})$ blocks. Since the factor $\log(\frac{T}{B})$ grows as the iterations progress, this implies that we are guaranteed to reach the number of blocks that is needed by our theory to imply convergence. However, since the factor grows slowly, we will not have to do too much unnecessary Cholesky factorizations before converging to a desired accuracy. Note that each Cholesky factor takes $O(s^2)$ memory, so if we store $O(\frac{n}{s} \log n)$ factors throughout the convergence, then this uses only $O(ns \log n)$ additional memory.

5.3 Symmetric Randomized Hadamard Transform

To ensure that uniformly sampled blocks yield a fast convergence rate for our algorithm, we must preprocess the linear system. Specifically, in the PSD case, where we assume that $\mathbf{A} = \Phi \Phi^\top$, we need to apply the randomized Hadamard transform \mathbf{Q} to Φ and \mathbf{b} , so that our theoretical analysis can be applied to the implicit block Kaczmarz algorithm based on (5.1). In the context of CD++, with access to \mathbf{A} and not Φ , this corresponds to transforming the original system into:

$$\mathbf{Q} \mathbf{A} \mathbf{Q}^\top \bar{\mathbf{x}} = \mathbf{Q} \mathbf{b}, \quad \mathbf{x} = \mathbf{Q}^\top \bar{\mathbf{x}},$$

where applying \mathbf{Q} on both sides of \mathbf{A} is crucial to maintaining the PSD structure of the system. Recall that the transform can be defined as $\mathbf{Q} = \mathbf{H} \mathbf{D}$, where $\mathbf{D} = \frac{1}{\sqrt{n}} \text{diag}(d_1, \dots, d_n)$ and d_i are independent random ± 1 signs (Rademacher variables). So, the dominant cost of this preprocessing step is applying the Hadamard transform \mathbf{H} on both sides of the matrix $\mathbf{D} \mathbf{A} \mathbf{D}$. The classical recursive algorithm for doing this, which we refer to as the Fast Hadamard Transform (FHT, see Appendix C), takes $mn \log n$ operations to compute $\text{FHT}(\mathbf{M}) = \mathbf{H} \mathbf{M}$ for an $n \times m$ matrix \mathbf{M} . Thus, the cost of computing $\mathbf{Q} \mathbf{A} \mathbf{Q}^\top = \text{FHT}(\text{FHT}(\mathbf{D} \mathbf{A} \mathbf{D})^\top)$ is roughly $2n^2 \log n$ operations. This suggests that, in order to maintain the positive definite structure for CD++, we must double the preprocessing cost compared to Kaczmarz++.

We show that this trade-off can be entirely avoided: By exploiting the symmetric structure of \mathbf{A} , we perform the two FHTs simultaneously at the cost of one FHT applied to a general matrix. We achieve this using a specialized recursive algorithm, which we call SymFHT (Algorithm 2). Here, for simplicity we write the recursion assuming that the input matrix is at least 2×2 . Naturally, the base case of the recursion is a 1×1 input matrix, in which case we let $\text{SymFHT}(\mathbf{A}) = \mathbf{A}$.

Note that, given an $n \times n$ matrix \mathbf{A} broken down into four $n/2 \times n/2$ blocks, the function SymFHT performs two recursive calls corresponding to the two diagonal blocks \mathbf{A}_{11} and \mathbf{A}_{22} , since both of these blocks are symmetric. The two off-diagonal blocks \mathbf{A}_{12} and \mathbf{A}_{12}^\top are not symmetric, so we must revert back to applying the classical FHT twice. But crucially, since the off-diagonal blocks are identical up to a transpose, we only have to transform one of them, which gives our recursion its computational gain, as shown in the following result. See Appendix C for proof.

Theorem 5.1. *Given an $n \times n$ symmetric matrix \mathbf{A} , where n is a power of 2, Algorithm 2 returns $\mathbf{H} \mathbf{A} \mathbf{H}$ after at most $n^2(2.5 + \log n)$ arithmetic operations.*

Algorithm 2 Symmetric Fast Hadamard Transform (SymFHT)

```

1: function SYMFHT(A)                                ▷ Input: Symmetric matrix  $\mathbf{A} = \begin{bmatrix} \mathbf{A}_{11} & \mathbf{A}_{12} \\ \mathbf{A}_{12}^\top & \mathbf{A}_{22} \end{bmatrix}$ .
2:   Compute  $\mathbf{B}_{11} \leftarrow \text{SymFHT}(\mathbf{A}_{11})$           ▷ Recursive call.
3:   Compute  $\mathbf{B}_{22} \leftarrow \text{SymFHT}(\mathbf{A}_{22})$           ▷ Recursive call.
4:   Compute  $\mathbf{B}_{12} \leftarrow \text{FHT}(\text{FHT}(\mathbf{A}_{12}^\top)^\top)$ 
5:   Compute  $\begin{bmatrix} \mathbf{C}_{11} & \mathbf{C}_{12} \\ \mathbf{C}_{21} & \mathbf{C}_{22} \end{bmatrix} \leftarrow \begin{bmatrix} \mathbf{B}_{11} + \mathbf{B}_{12}^\top & \mathbf{B}_{11} - \mathbf{B}_{12} \\ \mathbf{B}_{12} + \mathbf{B}_{22} & \mathbf{B}_{12}^\top - \mathbf{B}_{22} \end{bmatrix}$ 
6:
7:   return  $\begin{bmatrix} \mathbf{C}_{11} + \mathbf{C}_{21} & \mathbf{C}_{12} + \mathbf{C}_{22} \\ \mathbf{C}_{12}^\top + \mathbf{C}_{22}^\top & \mathbf{C}_{12} - \mathbf{C}_{22} \end{bmatrix}$           ▷ Computes HAH.
8: end function

```

5.4 Error Estimation and Adaptive Tuning

The remaining challenge with making our algorithms practical is effectively tracking the progress of the convergence, without spending significant additional computational cost. This progress tracking is important both for designing an effective stopping criterion for the algorithm, as well as to tune the acceleration parameters ρ and η .

Stopping criterion. Solvers such as CG commonly use a stopping criterion based on the relative residual error, i.e., $\|\mathbf{A}\mathbf{x}_t - \mathbf{b}\|/\|\mathbf{b}\| \leq \epsilon$ for some target value of ϵ . However, unlike in CG where the residual vector $\mathbf{A}\mathbf{x}_t - \mathbf{b}$ is computed as part of the method, in a Kaczmarz-type solver this vector is never explicitly computed, so using this stopping criterion directly would substantially add to the overall cost.

Instead, we propose to estimate the residual error by reusing the computations from the Kaczmarz updates. Specifically, in each update we compute the vector $\mathbf{r}_t = \mathbf{A}_{S_t}\mathbf{x}_t - \mathbf{b}_{S_t}$, which can be viewed as a sub-sample of the coordinates of $\bar{\mathbf{r}}_t = \mathbf{A}\mathbf{x}_t - \mathbf{b}$. Thus, we can use $\frac{n}{s}\|\mathbf{r}_t\|^2$ as a nearly-unbiased estimate of $\|\bar{\mathbf{r}}_t\|^2$ (the bias comes due to our block memoization scheme reusing previously sampled subsets; this bias is insignificant in practice). We propose to use a running average of these estimates:

$$\mathcal{E}_{t,p} = \frac{1}{p} \sum_{i=t-p}^t \frac{n}{s} \|\mathbf{A}_{S_i}\mathbf{x}_i - \mathbf{b}_{S_i}\|^2 \approx \|\mathbf{A}\mathbf{x}_t - \mathbf{b}\|^2. \quad (5.2)$$

This leads to our stopping criterion, $\mathcal{E}_{t,p} \leq \epsilon^2 \|\mathbf{b}\|^2$, where we let $p = n/s$, so that the estimate is most likely based on nearly all of the rows of \mathbf{A} (line 16 in Algorithm 3).

Acceleration Tuning. We next discuss how we can use runtime information to adaptively tune the acceleration parameters ρ and η . Recall from Theorem 2.1 that the momentum vector recursion $\mathbf{m}_{t+1} = \frac{1-\rho}{1+\rho}(\mathbf{m}_t - \mathbf{w}_t)$ is tied to its guaranteed expected convergence rate $\mathbb{E} \frac{\|\mathbf{x}_t - \mathbf{x}^*\|^2}{\|\mathbf{x}_0 - \mathbf{x}^*\|^2} \sim (1 - \rho/2)^t$ via the parameter ρ . A natural strategy is thus to use the algorithm's ongoing rate of convergence as a proxy for ρ , by comparing the residual norm estimates (5.2) at two different iterates.

Specifically, we propose to compute the ratio $r_{i,p} = \mathcal{E}_{t_i,p}/\mathcal{E}_{t_i-p,p} \approx \frac{\|\mathbf{A}\mathbf{x}_{t_i} - \mathbf{b}\|^2}{\|\mathbf{A}\mathbf{x}_{t_i-p} - \mathbf{b}\|^2}$ at certain checkpoints t_i during the run, and use them to recover a value of ρ that will be used in the momentum recursion. One possibility would be to simply let $\hat{\rho}_i = 1 - r_{i,p}^{1/p}$, which would give the most up-to-date convergence rate of the algorithm over the last p iterations until iteration t_i . However, this results

in a feedback loop, since the momentum recursion affects the convergence of the algorithm and vice versa, leading to the convergence rate oscillating up and down. To achieve stable convergence, we maintain a weighted average \hat{r}_i of the ratios $r_{i,p}$, and use $\hat{\rho}_i = 1 - \hat{r}_i^{1/p}$ (line 18). Concretely, we follow the parameter-free weighted averaging scheme proposed by [NDM23], which “forgets” older estimates quickly, while converging to a stable estimate:

$$\hat{r}_i = \frac{a_{t_i-1}}{a_{t_i}} \hat{r}_{i-1} + \left(1 - \frac{a_{t_i-1}}{a_{t_i}}\right) r_{i,p}, \quad \text{for } a_{t_i} = (i+1)^{\log(i+1)}. \quad (5.3)$$

Finally, we choose the momentum step size parameter η as indicated by our theory. From Theorem 2.1, we need $\eta = \Theta(\frac{1}{\nu})$ where ν is the variance parameter of the regularized projection. Then, using Theorem 3.7, we have that $\nu = \tilde{O}(\frac{n}{s})$, where s is the block size. This suggests $\eta \sim \frac{s}{n}$, and we simply set it to $\frac{s}{2n}$.

Combining the above ideas, we obtain CD++, given in Algorithm 3.

Algorithm 3 CD++: Coordinate descent solver for positive semidefinite systems

```

1: Input:  $\mathbf{A} \in \mathcal{S}_n^+$ ,  $\mathbf{b} \in \mathbb{R}^n$ , block size  $s$ , iterate  $\mathbf{x}_0$ , regularization  $\lambda$ , tolerance  $\epsilon$ ;
2: Sample  $\mathbf{D} \leftarrow \frac{1}{\sqrt{n}} \text{diag}(d_1, \dots, d_n)$  for  $d_i \sim \text{Rademacher}$ ;
3:  $\mathbf{A} \leftarrow \text{SymFHT}(\mathbf{DAD})$ ,  $\mathbf{b} \leftarrow \text{FHT}(\mathbf{Db})$ ; ▷ See Algorithm 2.
4: Initialize  $\mathbf{m}_0 \leftarrow \mathbf{0}$ ,  $\rho \leftarrow 0$ ,  $\eta \leftarrow \frac{s}{2n}$ ,  $\mathcal{B} \leftarrow \emptyset$ ,  $\tau \leftarrow \lceil n/s \rceil$ ,  $\mathcal{E}_0 \leftarrow \mathcal{E}_1 \leftarrow 0$ ,  $r \leftarrow 0$ ;
5: for  $t = 0, 1, \dots$  do
6:   if Bernoulli( $\min\{1, \frac{1}{t} \cdot \frac{n}{s} \log n\}$ ) then
7:      $\mathcal{B} \leftarrow \mathcal{B} \cup \{S\}$  for  $S \sim \binom{[n]}{s}$ ; ▷ Sample new subset.
8:      $\mathbf{R}[S] = \text{chol}(\mathbf{A}_{S,S} + \lambda \mathbf{I})$ ; ▷ Save Cholesky factor.
9:   else  $S \sim \mathcal{B}$ ; end if
10:   $\mathbf{r}_t \leftarrow \mathbf{A}_S \mathbf{x}_t - \mathbf{b}_S$ ; ▷ Use for error estimation.
11:   $\mathbf{w}_t \leftarrow \mathbf{I}_S^\top (\mathbf{A}_{S,S} + \lambda \mathbf{I})^{-1} \mathbf{r}_t$  using  $\mathbf{R}[S]$ ; ▷ Coordinate descent.
12:   $\mathbf{m}_{t+1} \leftarrow \frac{1-\rho}{1+\rho} (\mathbf{m}_t - \mathbf{w}_t)$ ; ▷ Adaptive momentum.
13:   $\mathbf{x}_{t+1} \leftarrow \mathbf{x}_t - \mathbf{w}_t + \eta \mathbf{m}_{t+1}$ ;
14:  if  $t < \tau \pmod{2\tau}$  then  $\mathcal{E}_0 \leftarrow \mathcal{E}_0 + \|\mathbf{r}_t\|^2$ ; else  $\mathcal{E}_1 \leftarrow \mathcal{E}_1 + \|\mathbf{r}_t\|^2$ ;
15:  if  $t = 2\tau - 1 \pmod{2\tau}$  then
16:    if  $\mathcal{E}_1 \leq \epsilon^2 \|\mathbf{b}\|^2$  then return  $\mathbf{D} \cdot \text{FHT}(\mathbf{x}_{t+1})$ ; ▷ Stopping criterion.
17:     $r \leftarrow r a_t + (\mathcal{E}_1 / \mathcal{E}_0)(1 - a_t)$ ; ▷ Weighted average (5.3).
18:     $\rho \leftarrow 1 - r^{1/\tau}$ ; ▷ Convergence rate estimate.
19:     $\mathcal{E}_0 \leftarrow \mathcal{E}_1 \leftarrow 0$ ;
20:  end if
21: end for

```

6 Numerical Experiments

In this section, we present numerical experiments that support our theory. First, we demonstrate that the convergence analysis carried out in Sections 2-4 accurately predicts the performance of Kaczmarz++/CD++, by evaluating the effect of adaptive acceleration, block memoization and regularized projections on their convergence rate. Then, we compare our methods to popular Krylov solvers, CG [HS52] and GMRES [SS86], showing that the Kaczmarz++ framework achieves better computational cost for certain classes of linear systems that arise naturally in applications such as machine learning, as suggested by our theory.

6.1 Experimental Setup

We set up our experiments to evaluate how well the solvers exploit large outlying singular values to achieve fast convergence for ill-conditioned systems. To that end, we consider two families of positive semidefinite linear systems which naturally exhibit such spectral structure, resulting in 20 different linear system tasks (see Appendix D for formal definitions).

Synthetic Low-Rank Matrices. To gain precise control on the eigenvalue distribution of the system, we first consider a collection of synthetic benchmark matrices with a bell-shaped spectrum, constructed via the `make_low_rank_matrix` function in Scikit-learn [PVG⁺11]. We control the number of large outlying eigenvalues via the function parameter `effective_rank`, choosing among four values (25, 50, 100, and 200).

Kernel Matrices from Machine Learning. We also consider four real-world benchmark datasets, available through Scikit-learn [PVG⁺11] and OpenML [VvRBT13]: Abalone, California.housing, Covtype, and Phoneme. We transform these datasets using a kernel function to produce a PSD kernel matrix. For the kernel function, we consider two types of radial basis functions (Gaussian and Laplacian), each with two different values of width $\gamma \in \{0.1, 0.01\}$. These are known to produce highly ill-conditioned matrices with fast spectral decays, leading to many large outlying eigenvalues [RW06].

Each resulting PSD matrix \mathbf{A} is truncated to dimensions 4096×4096 . Then, following standard applications in Kernel Ridge Regression [AM15], for each matrix we define a regularized linear system $(\mathbf{A} + \phi\mathbf{I})\mathbf{x} = \mathbf{b}$, where \mathbf{b} is a standard Gaussian vector and $\phi = 0.001$. We evaluate the returned solutions via the normalized residual:

$$\epsilon = \|(\mathbf{A} + \phi\mathbf{I})\mathbf{x} - \mathbf{b}\|/\|\mathbf{b}\|. \tag{6.1}$$

6.2 Verifying Our Convergence Analysis

To verify our convergence analysis, we implement four variants of our algorithms and plot the per-iteration convergence on all tasks (details in Appendix D).

Since the tasks are all positive semidefinite, we focus on CD++ (Algorithm 3). To isolate the effect of its individual components, such as block size, acceleration, and memoization, we consider four variants of the method that toggle acceleration and memoization on/off, as illustrated in Table 1, each with four different block sizes (25, 50, 100, and 200). In particular, no memoization means that we sample a new block set S uniformly at random from $\binom{[n]}{s}$ at every step (and compute its Cholesky factor), while no acceleration means setting the momentum step size η to 0. We show convergence plots for synthetic matrices with effective rank 100 and 200 in Figure 1, and include the remaining 6 plots (2 for synthetic matrices and 4 for the Abalone dataset) in Figure 3 of Appendix D.

Solver	Accelerate	Memoize
CD	✗	✗
CD+Accel	✓	✗
CD+Memo	✗	✓
Full CD++	✓	✓

Table 1: Implemented variants of CD++.

Block size. First, observe that as we increase the block size, all of the methods achieve faster per-iteration convergence rate, as expected from our theory. Looking closely, we can see that this rate improves more than just proportionally to the increase in block size, which means that larger blocks lead to greater efficiency in terms of how many rows of \mathbf{A} need to be processed by the algorithm to

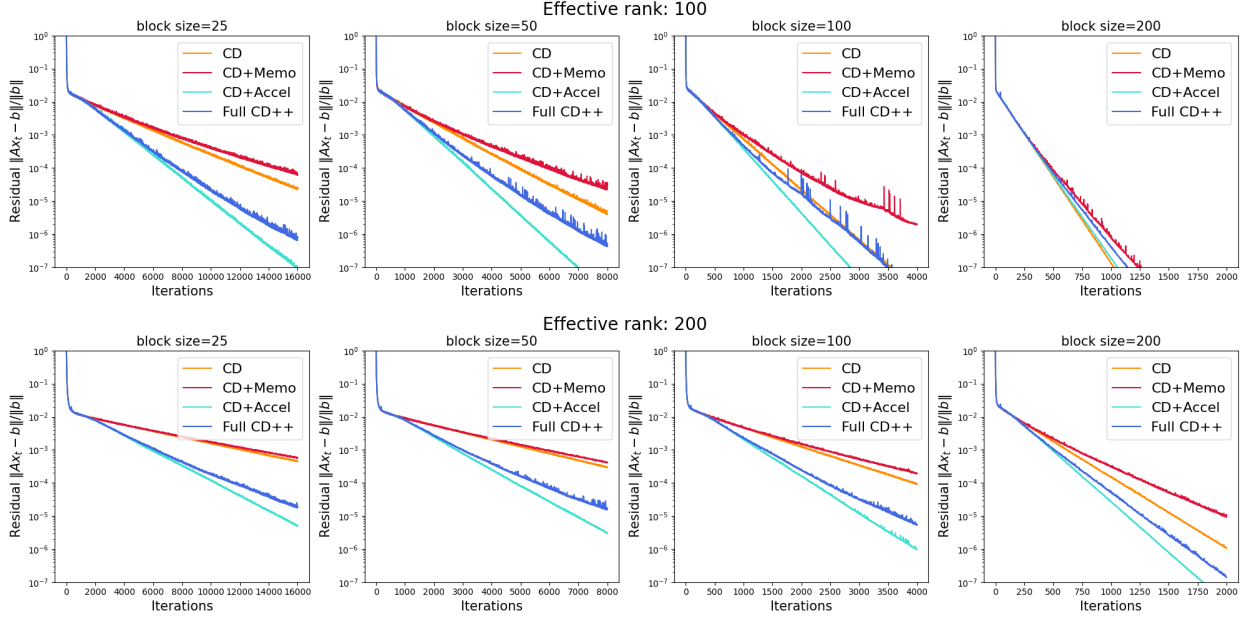


Figure 1: Convergence plots for different variants of CD++ (see Table 1) using four block sizes (25, 50, 100, and 200), on synthetic test matrices with effective rank 100 (top) and 200 (bottom). Note that the iterations range in each column is scaled to keep $(iterations \times block-size)$ consistent.

reach certain accuracy. This corresponds to the $\bar{\kappa}_k$ condition number in our theory, which decreases as the block size increases, indicating that the methods do exploit large outlying eigenvalues. Also, as we increase the effective rank of the matrix (i.e., the number of large eigenvalues, corresponds to k in our theory), we need larger block sizes to attain fast convergence.

Adaptive acceleration. Comparing CD and CD+Accel, we see that our adaptive acceleration significantly improves the convergence rate, particularly for small-to-moderate block sizes. However, when the block size is much larger than the effective rank, then the benefit of acceleration will necessarily be reduced (top right plot), because in this case the condition number $\bar{\kappa}_k$ is just a small constant.

Block memoization. Comparing CD+Accel and Full CD++, we see that introducing our block memoization scheme (i.e., sampling from a small collection of random blocks) only slightly reduces the per-iteration convergence rate compared to the method that samples a new random block at every step. This is explained by our analysis in Theorem 4.2. The benefits of block memoization become apparent once we compare the computational cost of both procedures, as discussed below (Figure 2).

Regularized projections. In Appendix D.3, we tested Full CD++ with different choices of the projection regularizer λ . In all our experiments, the convergence remained largely unchanged for any $\lambda \in [0, 0.01]$ (note that our theory requires $\lambda > 0$). This suggests that regularizing the Kaczmarz projection can be done without sacrificing the convergence, and so, we recommend using CD++ with a small but positive λ to ensure stable computation of the Cholesky factors (we used $\lambda = 10^{-8}$ as a default).

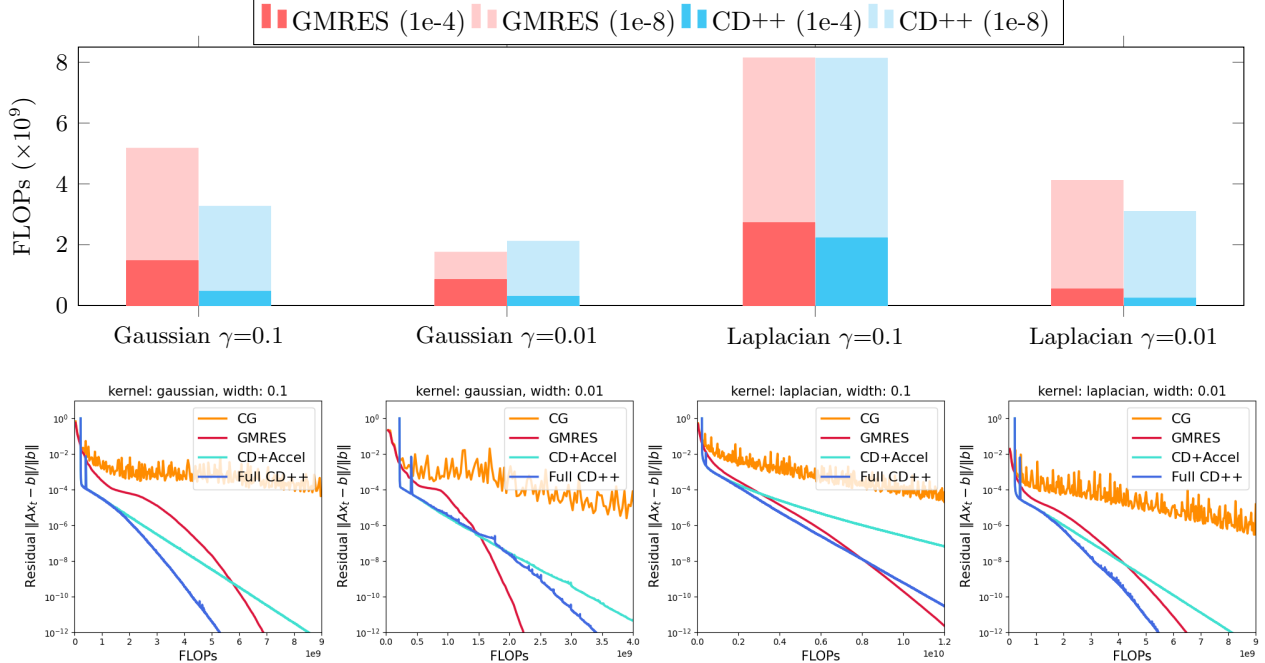


Figure 2: Computational cost comparison, measuring floating point operations (FLOPs) needed to reach a given error threshold on four kernel matrices constructed from the Abalone dataset. Above, we show total FLOPs for GMRES and CD++ to reach one of two error thresholds, $\epsilon \in \{10^{-4}, 10^{-8}\}$. Below, we show convergence-vs-FLOPs plots, including CG and CD+Accel as additional baselines.

6.3 Comparison with Krylov Subspace Methods

Next, we evaluate the computational cost of our methods, comparing them to Krylov solvers. Specifically, we count floating point operations (FLOPs) needed to reach a given error threshold. Here, we show the results for kernel matrices obtained from the Abalone dataset, while results for the remaining test matrices are in Appendix D.2.

In Figure 2 (bottom) we show the convergence plots of the methods, with FLOPs instead of iterations on the x-axis (for our methods, this includes the cost of RHT pre-processing). We again compare Full CD++ and CD+Accel (i.e., Algorithm 3 with and without block memoization, using block size 200). We see that, even though block memoization slightly reduces the per-iteration convergence (Figure 1), it more than makes up for this in the computations. In particular, Full CD++ exhibits a phase transition where it accelerates past CD+Accel once enough blocks have been memoized and it no longer pays for the block Cholesky factorizations (e.g., see bottom left plot in Figure 2).

We compare the computational cost of CD++ with two Krylov solvers, CG and GMRES. First, we observe that CG struggles to converge on all of the tested matrices. This suggests that the systems are indeed ill-conditioned, and CG cannot overcome this effectively due to numerical stability issues. On the other hand, GMRES avoids these issues by maintaining an explicit Krylov basis, and thus after a number of initial iterations, it exploits the large outlying eigenvalues to achieve fast convergence.

Thus, in most cases, both CD++ and GMRES exhibit two distinct phases of convergence, as suggested by the theory. However, in the majority of our test cases, the second phase of CD++ starts sooner than for GMRES, matching our complexity analysis from equations (1.1) and (1.3). This gives CD++ a computational advantage over GMRES, particularly in the low-to-moderate

precision regime (say, $\epsilon > 10^{-6}$). In the high precision regime (say, $\epsilon < 10^{-6}$), CD++ maintains its fast convergence, while GMRES, in some cases, further accelerates by exploiting smaller isolated eigenvalues.

These overall trends are reflected in Figure 2 (top), showing the total FLOP counts of GMRES and CD++ with two error thresholds, $\epsilon \in \{10^{-4}, 10^{-8}\}$. We see that for $\epsilon = 10^{-4}$, CD++ is consistently more efficient than GMRES, while for $\epsilon = 10^{-8}$, GMRES overtakes CD++ in some cases. Across all tested matrices (see Appendix D.2 for details), we observed that for $\epsilon = 10^{-4}$, CD++ performed better than GMRES in 18 out of 20 cases, while for $\epsilon = 10^{-8}$, it did so in 14 out of 20 cases.

7 Conclusions

We developed new Kaczmarz methods, called Kaczmarz++ and CD++, which exploit large outlying singular values to attain fast convergence in solving many ill-conditioned linear systems. We demonstrated both theoretically and empirically that our methods outperform Krylov solvers such as CG and GMRES on certain classes of problems that arise naturally, for instance, in the machine learning literature. Along the way, we introduced and analyzed several novel algorithmic techniques to the Kaczmarz framework, including adaptive acceleration, regularized projections and block memoization.

A potential future direction is to develop Kaczmarz-type methods that can exploit not just large but also small isolated singular values to achieve fast convergence, as motivated by applications in partial differential equations, among others. Another natural question is whether it is possible to adapt Krylov subspace methods to take advantage of row-sampling techniques in order to improve their computational guarantees beyond what is possible through only matrix-vector products.

Acknowledgments

Thanks to Daniel LeJeune for helpful discussions regarding accelerated sketch-and-project, and for sharing the programming environment. Also, thanks to Sachin Garg for helpful discussions on block memoization.

References

- [AC09] Nir Ailon and Bernard Chazelle. The fast Johnson–Lindenstrauss transform and approximate nearest neighbors. *SIAM Journal on Computing*, 39(1):302–322, 2009.
- [ACW17] Haim Avron, Kenneth L Clarkson, and David P Woodruff. Faster kernel ridge regression using sketching and preconditioning. *SIAM Journal on Matrix Analysis and Applications*, 38(4):1116–1138, 2017.
- [AL86] Owe Axelsson and Gunhild Lindskog. On the rate of convergence of the preconditioned conjugate gradient method. *Numerische Mathematik*, 48:499–523, 1986.
- [ALM24] Seth J Alderman, Roan W Luikart, and Nicholas F Marshall. Randomized kaczmarz with geometrically smoothed momentum. *SIAM Journal on Matrix Analysis and Applications*, 45(4):2287–2313, 2024.
- [AM15] Ahmed Alaoui and Michael W Mahoney. Fast randomized kernel ridge regression with statistical guarantees. *Advances in Neural Information Processing Systems*, 28, 2015.

- [AMT10] Haim Avron, Petar Maymounkov, and Sivan Toledo. Blendenpik: Supercharging lapack’s least-squares solver. *SIAM Journal on Scientific Computing*, 32(3):1217–1236, 2010.
- [CDDR24] Shabarish Chenakkod, Michał Dereziński, Xiaoyu Dong, and Mark Rudelson. Optimal embedding dimension for sparse subspace embeddings. In *56th ACM Symposium on Theory of Computing*, 2024.
- [CW13] Kenneth L Clarkson and David P Woodruff. Low rank approximation and regression in input sparsity time. In *45th ACM Symposium on Theory of Computing*, pages 81–90, 2013.
- [DKM20] Michał Dereziński, Rajiv Khanna, and Michael W Mahoney. Improved guarantees and a multiple-descent curve for column subset selection and the Nyström method. *Advances in Neural Information Processing Systems*, 33:4953–4964, 2020.
- [DLM20] Michał Dereziński, Feynman Liang, and Michael Mahoney. Bayesian experimental design using regularized determinantal point processes. In *International Conference on Artificial Intelligence and Statistics*, pages 3197–3207. PMLR, 2020.
- [DLNR24] Michał Dereziński, Daniel LeJeune, Deanna Needell, and Elizaveta Rebrova. Fine-grained analysis and faster algorithms for iteratively solving linear systems. *arXiv preprint arXiv:2405.05818*, 2024.
- [DM16] Petros Drineas and Michael W Mahoney. RandNLA: randomized numerical linear algebra. *Communications of the ACM*, 59(6):80–90, 2016.
- [DM21] Michał Dereziński and Michael W Mahoney. Determinantal point processes in randomized numerical linear algebra. *Notices of the American Mathematical Society*, 68(1):34–45, 2021.
- [DM24] Michał Dereziński and Michael W Mahoney. Recent and upcoming developments in randomized numerical linear algebra for machine learning. In *Proceedings of the 30th ACM SIGKDD Conference on Knowledge Discovery and Data Mining*, pages 6470–6479, 2024.
- [DR24] Michał Dereziński and Elizaveta Rebrova. Sharp analysis of sketch-and-project methods via a connection to randomized singular value decomposition. *SIAM Journal on Mathematics of Data Science*, 6(1):127–153, 2024.
- [DY24] Michał Dereziński and Jiaming Yang. Solving dense linear systems faster than via preconditioning. In *56th Annual ACM Symposium on Theory of Computing*, 2024.
- [EGW24] Ethan N Epperly, Gil Goldshlager, and Robert J Webber. Randomized kaczmarz with tail averaging. *arXiv preprint arXiv:2411.19877*, 2024.
- [EHL81] Paulus Petrus Bernardus Eggermont, Gabor T Herman, and Arnold Lent. Iterative algorithms for large partitioned linear systems, with applications to image reconstruction. *Linear algebra and its applications*, 40:37–67, 1981.
- [Elf80] Tommy Elfving. Block-iterative methods for consistent and inconsistent linear equations. *Numerische Mathematik*, 35:1–12, 1980.

- [FCM⁺92] Hans Georg Feichtinger, C Cenker, M Mayer, H Steier, and Thomas Strohmer. New variants of the pocs method using affine subspaces of finite codimension with applications to irregular sampling. In *Visual Communications and Image Processing*, volume 1818, pages 299–310, 1992.
- [FTU23] Zachary Frangella, Joel A Tropp, and Madeleine Udell. Randomized Nyström preconditioning. *SIAM Journal on Matrix Analysis and Applications*, 44(2):718–752, 2023.
- [GHR18] Robert Gower, Filip Hanzely, Peter Richtárik, and Sebastian U Stich. Accelerated stochastic matrix inversion: general theory and speeding up BFGS rules for faster second-order optimization. *Advances in Neural Information Processing Systems*, 31, 2018.
- [GR15] Robert M Gower and Peter Richtárik. Randomized iterative methods for linear systems. *SIAM Journal on Matrix Analysis and Applications*, 36(4):1660–1690, 2015.
- [HM93] Gabor T Herman and Lorraine B Meyer. Algebraic reconstruction techniques can be made computationally efficient (positron emission tomography application). *IEEE transactions on medical imaging*, 12(3):600–609, 1993.
- [HNR17] Ahmed Hefny, Deanna Needell, and Aaditya Ramdas. Rows versus columns: Randomized kaczmarz or gauss-seidel for ridge regression. *SIAM Journal of Scientific Computing*, 39(5):S528–S542, 2017.
- [HS52] Magnus Rudolph Hestenes and Eduard Stiefel. *Methods of conjugate gradients for solving linear systems*, volume 49. NBS Washington, DC, 1952.
- [Kac37] S. Kaczmarz. Angenäherte auflösung von systemen linearer gleichungen. *Bull. Int. Acad. Polon. Sci. Lett. Ser. A*, pages 335–357, 1937.
- [LR24] Jackie Lok and Elizaveta Rebrova. A subspace constrained randomized Kaczmarz method for structure or external knowledge exploitation. *Linear Algebra and its Applications*, 2024.
- [MN22] Maike Meier and Yuji Nakatsukasa. Randomized algorithms for tikhonov regularization in linear least squares. *arXiv preprint arXiv:2203.07329*, 2022.
- [MSM14] Xiangrui Meng, Michael A Saunders, and Michael W Mahoney. Lsrn: A parallel iterative solver for strongly over-or underdetermined systems. *SIAM Journal on Scientific Computing*, 36(2):C95–C118, 2014.
- [MT20] Per-Gunnar Martinsson and Joel A Tropp. Randomized numerical linear algebra: Foundations and algorithms. *Acta Numerica*, 29:403–572, 2020.
- [Nat01] Frank Natterer. *The mathematics of computerized tomography*. SIAM, 2001.
- [NDM23] Sen Na, Michał Dereziński, and Michael W Mahoney. Hessian averaging in stochastic newton methods achieves superlinear convergence. *Mathematical Programming*, 201(1):473–520, 2023.
- [Nes13] Yurii Nesterov. *Introductory lectures on convex optimization: A basic course*, volume 87. Springer Science & Business Media, 2013.

- [NT14] Deanna Needell and Joel A Tropp. Paved with good intentions: analysis of a randomized block Kaczmarz method. *Linear Algebra and its Applications*, 441:199–221, 2014.
- [NWS14] Deanna Needell, Rachel Ward, and Nati Srebro. Stochastic gradient descent, weighted sampling, and the randomized Kaczmarz algorithm. *Advances in neural information processing systems*, 27, 2014.
- [Pet15] Stefania Petra. Randomized sparse block kaczmarz as randomized dual block-coordinate descent. *Analele stiintifice ale Universitatii Ovidius Constanta. Seria Matematica*, 23(3):129–149, 2015.
- [PJM23] Vivak Patel, Mohammad Jahangoshahi, and D Adrian Maldonado. Randomized block adaptive linear system solvers. *SIAM Journal on Matrix Analysis and Applications*, 44(3):1349–1369, 2023.
- [PS82] Christopher C Paige and Michael A Saunders. LSQR: An algorithm for sparse linear equations and sparse least squares. *ACM Transactions on Mathematical Software (TOMS)*, 8(1):43–71, 1982.
- [PVG⁺11] F. Pedregosa, G. Varoquaux, A. Gramfort, V. Michel, B. Thirion, O. Grisel, M. Blondel, P. Prettenhofer, R. Weiss, V. Dubourg, J. Vanderplas, A. Passos, D. Cournapeau, M. Brucher, M. Perrot, and E. Duchesnay. Scikit-learn: Machine learning in Python. *Journal of Machine Learning Research*, 12:2825–2830, 2011.
- [RN21] Elizaveta Rebrova and Deanna Needell. On block Gaussian sketching for the Kaczmarz method. *Numerical Algorithms*, 86:443–473, 2021.
- [RW06] C. E. Rasmussen and C. K. I. Williams. *Gaussian Processes for Machine Learning*. MIT Press, 2006.
- [SS86] Youcef Saad and Martin H Schultz. GMRES: A generalized minimal residual algorithm for solving nonsymmetric linear systems. *SIAM Journal on scientific and statistical computing*, 7(3):856–869, 1986.
- [SV09] T. Strohmer and R. Vershynin. A randomized Kaczmarz algorithm with exponential convergence. *J. Fourier Anal. Appl.*, 15(2):262–278, 2009.
- [Tro11] Joel A Tropp. Improved analysis of the subsampled randomized Hadamard transform. *Advances in Adaptive Data Analysis*, 3(01n02):115–126, 2011.
- [Tro15] Joel A. Tropp. An introduction to matrix concentration inequalities. *Foundations and Trends[®] in Machine Learning*, 8(1-2):1–230, 2015.
- [VvRBT13] Joaquin Vanschoren, Jan N. van Rijn, Bernd Bischl, and Luis Torgo. Openml: Networked science in machine learning. *SIGKDD Explorations*, 15(2):49–60, 2013.

A Acceleration Analysis: Proofs of Lemmas 2.3 and 2.4

A.1 Proof of Lemma 2.3

Proof of Lemma 2.3. First, we show that $1 \leq \nu \leq 1/\mu$. This follows since:

$$\begin{aligned} 1 &= \|(\bar{\mathbf{P}}_\lambda^{\dagger/2} \mathbb{E}[\mathbf{P}_{\lambda,S}] \bar{\mathbf{P}}_\lambda^{\dagger/2})^2\| \leq \|\mathbb{E}[(\bar{\mathbf{P}}_\lambda^{\dagger/2} \mathbf{P}_{\lambda,S} \bar{\mathbf{P}}_\lambda^{\dagger/2})^2]\| = \nu, \\ \nu &\leq \|\bar{\mathbf{P}}_\lambda^\dagger\| \|\bar{\mathbf{P}}_\lambda^{\dagger/2} \mathbb{E}[\mathbf{P}_{\lambda,S}^2] \bar{\mathbf{P}}_\lambda^{\dagger/2}\| \leq \|\bar{\mathbf{P}}_\lambda^\dagger\| = 1/\mu, \end{aligned}$$

where we used Jensen's inequality and that $\mathbf{P}_{\lambda,S} \preceq \mathbf{I}$.

Our proof of the convergence guarantee follows closely the steps of [DLNR24], who introduced inexact updates into the argument of [GHR18]. Denote $\mathbf{e}_t := \tilde{\mathbf{w}}_t - \mathbf{w}_t$ as the approximation error, and denote $\mathbf{v}_{t+1}^* := \mathbf{v}_{t+1} + \gamma \tilde{\mathbf{w}}_t - \gamma \mathbf{w}_t = \mathbf{v}_{t+1} + \gamma \mathbf{e}_t$ as the exact update. Let $\mathbf{r}_t := \|\mathbf{v}_t - \mathbf{x}^*\|_{\bar{\mathbf{P}}_\lambda^\dagger}$ and $\mathbf{r}_t^* := \|\mathbf{v}_t^* - \mathbf{x}^*\|_{\bar{\mathbf{P}}_\lambda^\dagger}$ where $\bar{\mathbf{P}}_\lambda = \mathbb{E}[\mathbf{P}_{\lambda,S}]$. We have the following:

$$\begin{aligned} \mathbb{E}[\mathbf{r}_{t+1}^2] &= \mathbb{E}[\|\mathbf{v}_{t+1} - \mathbf{x}^*\|_{\bar{\mathbf{P}}_\lambda^\dagger}^2] = \mathbb{E}[\|\mathbf{v}_{t+1}^* - \mathbf{x}^* - \gamma \mathbf{e}_t\|_{\bar{\mathbf{P}}_\lambda^\dagger}^2] \\ &\leq (1 + \phi) \mathbb{E}[(\mathbf{r}_{t+1}^*)^2] + (1 + \frac{1}{\phi}) \mathbb{E}[\|\gamma \mathbf{e}_t\|_{\bar{\mathbf{P}}_\lambda^\dagger}^2], \end{aligned} \tag{A.1}$$

where we use the fact that $\phi a^2 + \frac{1}{\phi} b^2 \geq 2ab$ for $\phi > 0$, and we will specify ϕ later. According to Appendix A.3 in [GHR18], we can decompose $(\mathbf{r}_{t+1}^*)^2$ into three parts:

$$\begin{aligned} (\mathbf{r}_{t+1}^*)^2 &= \underbrace{\|\beta \mathbf{v}_t + (1 - \beta) \mathbf{x}_t - \mathbf{x}^*\|_{\bar{\mathbf{P}}_\lambda^\dagger}^2}_I + \underbrace{\gamma^2 \|\mathbf{P}_{\lambda,S} (\mathbf{x}_t - \mathbf{x}^*)\|_{\bar{\mathbf{P}}_\lambda^\dagger}^2}_{II} \\ &\quad - 2\gamma \underbrace{\left\langle \beta (\mathbf{v}_t - \mathbf{x}^*) + (1 - \beta) (\mathbf{x}_t - \mathbf{x}^*), \bar{\mathbf{P}}_\lambda^\dagger \mathbf{P}_{\lambda,S} (\mathbf{x}_t - \mathbf{x}^*) \right\rangle}_{III} \end{aligned}$$

We upper bound the three terms separately. For the first term, following [GHR18] and with the use of a parallelogram identity, we have

$$I = \|\beta (\mathbf{v}_t - \mathbf{x}^*) + (1 - \beta) (\mathbf{x}_t - \mathbf{x}^*)\|_{\bar{\mathbf{P}}_\lambda^\dagger}^2 \leq \beta \mathbf{r}_t^2 + (1 - \beta) \|\mathbf{x}_t - \mathbf{x}^*\|_{\bar{\mathbf{P}}_\lambda^\dagger}^2.$$

For the second term, since $\nu \leq \tilde{\nu}$, we have

$$\begin{aligned} \mathbb{E}[II \mid \mathbf{x}_t] &= \mathbb{E}[\|\mathbf{P}_{\lambda,S} (\mathbf{x}_t - \mathbf{x}^*)\|_{\bar{\mathbf{P}}_\lambda^\dagger}^2 \mid \mathbf{x}_t] = \left\langle \mathbb{E}[\mathbf{P}_{\lambda,S} \bar{\mathbf{P}}_\lambda^\dagger \mathbf{P}_{\lambda,S}] (\mathbf{x}_t - \mathbf{x}^*), (\mathbf{x}_t - \mathbf{x}^*) \right\rangle \\ &\leq \nu \cdot \langle \bar{\mathbf{P}}_\lambda (\mathbf{x}_t - \mathbf{x}^*), \mathbf{x}_t - \mathbf{x}^* \rangle \leq \tilde{\nu} \cdot \|\mathbf{x}_t - \mathbf{x}^*\|_{\bar{\mathbf{P}}_\lambda}^2 \end{aligned}$$

where in the third step we use the definition of ν . For the third term we have

$$\begin{aligned} \mathbb{E}[III \mid \mathbf{x}_t, \mathbf{v}_t, \mathbf{y}_t] &= \left\langle \beta \mathbf{v}_t + (1 - \beta) \mathbf{x}_t - \mathbf{x}^*, \bar{\mathbf{P}}_\lambda^\dagger \bar{\mathbf{P}}_\lambda (\mathbf{x}_t - \mathbf{x}^*) \right\rangle \\ &= \langle \beta \mathbf{v}_t + (1 - \beta) \mathbf{x}_t - \mathbf{x}^*, \mathbf{x}_t - \mathbf{x}^* \rangle \\ &= \left\langle \mathbf{x}_t - \mathbf{x}^* + \frac{\beta(1 - \alpha)}{\alpha} (\mathbf{x}_t - \mathbf{y}_t), \mathbf{x}_t - \mathbf{x}^* \right\rangle \\ &= \|\mathbf{x}_t - \mathbf{x}^*\|^2 - \frac{\beta(1 - \alpha)}{2\alpha} (\|\mathbf{y}_t - \mathbf{x}^*\|^2 - \|\mathbf{x}_t - \mathbf{y}_t\|^2 - \|\mathbf{x}_t - \mathbf{x}^*\|^2) \end{aligned}$$

where the second step follows from the assumption that $\mathbf{x}_t - \mathbf{x}^* \in \text{range}(\bar{\mathbf{P}}_\lambda)$ and also the property of pseudoinverse that $\bar{\mathbf{P}}_\lambda^\dagger \bar{\mathbf{P}}_\lambda \mathbf{w} = \mathbf{w}$ for any $\mathbf{w} \in \text{range}(\bar{\mathbf{P}}_\lambda)$, the third step follows from the first equation of (2.2) and the last step follows from the parallelogram identity. Moreover, by using the fact that $\mathbf{P}_{\lambda,S}^2 \preceq \mathbf{P}_{\lambda,S}$ we have

$$\begin{aligned} \mathbb{E} \left[\|\mathbf{y}_{t+1} - \mathbf{x}^*\|^2 \mid \mathbf{x}_t \right] &= \mathbb{E} \left[\|(\mathbf{I} - \mathbf{P}_{\lambda,S})(\mathbf{x}_t - \mathbf{x}^*) - \mathbf{e}_t\|^2 \mid \mathbf{x}_t \right] \\ &\leq (1 + \phi) \langle (\mathbf{I} - \bar{\mathbf{P}}_\lambda)(\mathbf{x}_t - \mathbf{x}^*), \mathbf{x}_t - \mathbf{x}^* \rangle + \left(1 + \frac{1}{\phi}\right) \mathbb{E}[\|\mathbf{e}_t\|^2] \\ &= (1 + \phi) \left(\|\mathbf{x}_t - \mathbf{x}^*\|^2 - \|\mathbf{x}_t - \mathbf{x}^*\|_{\bar{\mathbf{P}}_\lambda}^2 \right) + \left(1 + \frac{1}{\phi}\right) \mathbb{E}[\|\mathbf{e}_t\|^2]. \end{aligned}$$

By combining the above four bounds, we have the following bound for $\mathbb{E}[(\mathbf{r}_{t+1}^*)^2]$:

$$\begin{aligned} &\mathbb{E}[(\mathbf{r}_{t+1}^*)^2] \\ &= I + \gamma^2 \mathbb{E}[II \mid \mathbf{x}_t] - 2\gamma \mathbb{E}[III \mid \mathbf{x}_t, \mathbf{v}_t, \mathbf{y}_t] \\ &\leq \beta \mathbf{r}_t^2 + (1 - \beta) \|\mathbf{x}_t - \mathbf{x}^*\|_{\bar{\mathbf{P}}_\lambda^\dagger}^2 + \gamma^2 \tilde{\nu} \|\mathbf{x}_t - \mathbf{x}^*\|_{\bar{\mathbf{P}}_\lambda}^2 \\ &\quad - 2\gamma \left(\|\mathbf{x}_t - \mathbf{x}^*\|^2 - \frac{\beta(1 - \alpha)}{2\alpha} (\|\mathbf{y}_t - \mathbf{x}^*\|^2 - \|\mathbf{x}_t - \mathbf{y}_t\|^2 - \|\mathbf{x}_t - \mathbf{x}^*\|^2) \right) \\ &\leq \beta \mathbf{r}_t^2 + \frac{1 - \beta}{\tilde{\mu}} \|\mathbf{x}_t - \mathbf{x}^*\|^2 \\ &\quad + \gamma^2 \tilde{\nu} \left(\|\mathbf{x}_t - \mathbf{x}^*\|^2 - \frac{1}{1 + \phi} \mathbb{E} \left[\|\mathbf{y}_{t+1} - \mathbf{x}^*\|^2 \mid \mathbf{x}_t \right] + \frac{1 + 1/\phi}{1 + \phi} \mathbb{E}[\|\mathbf{e}_t\|^2] \right) \\ &\quad - 2\gamma \left(\|\mathbf{x}_t - \mathbf{x}^*\|^2 - \frac{\beta(1 - \alpha)}{2\alpha} (\|\mathbf{y}_t - \mathbf{x}^*\|^2 - \|\mathbf{x}_t - \mathbf{x}^*\|^2) \right) \end{aligned} \tag{A.2}$$

where in the last step we use the fact that $\|\bar{\mathbf{P}}_\lambda^\dagger\| \leq 1/\mu$ and $\mu \geq \tilde{\mu}$. For the bound on $\mathbf{e}_t = \tilde{\mathbf{w}}_t - \mathbf{w}_t$, supposing that $\|\mathbf{e}_t\| \leq \epsilon_1 \|\mathbf{w}_t\|$, we have

$$\mathbb{E}[\|\mathbf{e}_t\|^2] \leq \epsilon_1^2 \mathbb{E}[\|\mathbf{w}_t\|^2] = \epsilon_1^2 \mathbb{E}[\|\mathbf{P}_{\lambda,S}(\mathbf{x}_t - \mathbf{x}^*)\|^2] \leq \epsilon_1^2 \|\bar{\mathbf{P}}_\lambda\| \cdot \|\mathbf{x}_t - \mathbf{x}^*\|^2 \tag{A.3}$$

and also

$$\mathbb{E}[\|\mathbf{e}_t\|_{\bar{\mathbf{P}}_\lambda^\dagger}^2] \leq \|\bar{\mathbf{P}}_\lambda^\dagger\| \cdot \mathbb{E}[\|\mathbf{e}_t\|^2] \leq \frac{\epsilon_1^2 \|\bar{\mathbf{P}}_\lambda\|}{\tilde{\mu}} \cdot \|\mathbf{x}_t - \mathbf{x}^*\|^2 \tag{A.4}$$

Finally, by combining (A.1), (A.2), (A.3) and (A.4) we have

$$\begin{aligned} &\mathbb{E}[\mathbf{r}_{t+1}^2 + \gamma^2 \tilde{\nu} \|\mathbf{y}_{t+1} - \mathbf{x}^*\|^2] \\ &\leq (1 + \phi) \mathbb{E}[(\mathbf{r}_{t+1}^*)^2] + (1 + \frac{1}{\phi}) \mathbb{E}[\|\gamma \mathbf{e}_t\|_{\bar{\mathbf{P}}_\lambda^\dagger}^2] + \gamma^2 \tilde{\nu} \mathbb{E}[\|\mathbf{y}_{t+1} - \mathbf{x}^*\|^2] \\ &\leq (1 + \phi) \beta \mathbf{r}_t^2 + \beta(1 + \phi) \underbrace{\frac{\gamma(1 - \alpha)}{\alpha}}_{P_1} \|\mathbf{y}_t - \mathbf{x}^*\|^2 \\ &\quad + (1 + \phi) \underbrace{\left(\frac{1 - \beta}{\tilde{\mu}} + \gamma^2 \tilde{\nu} - 2\gamma - \frac{\gamma\beta(1 - \alpha)}{\alpha} + \frac{\gamma^2 \epsilon_1^2 \|\bar{\mathbf{P}}_\lambda\|}{\phi} (\tilde{\nu} + \frac{1}{\tilde{\mu}}) \right)}_{P_2} \|\mathbf{x}_t - \mathbf{x}^*\|^2. \end{aligned}$$

By choosing $\alpha = \frac{1}{1+\gamma\tilde{\nu}}$ and $\gamma = \frac{1}{\sqrt{\tilde{\nu}\tilde{\mu}}}$ we have $P_1 = \gamma^2\tilde{\nu} = \frac{1}{\tilde{\mu}}$. By choosing $\beta = 1 - \sqrt{\frac{\tilde{\mu}}{\tilde{\nu}}}$ we have $\beta(1+\phi) \leq 1 - \frac{1}{2}\sqrt{\frac{\tilde{\mu}}{\tilde{\nu}}}$ holds for $\phi = \frac{\sqrt{\tilde{\mu}/\tilde{\nu}}}{2(1-\sqrt{\tilde{\mu}/\tilde{\nu}})}$. By further setting $\epsilon_1 \leq \frac{\tilde{\mu}}{4} \leq \frac{\tilde{\mu}}{\sqrt{8\|\mathbf{P}_\lambda\|(\tilde{\mu}\tilde{\nu}+1)}}$ we also achieve $P_2 \leq 0$. Finally, denote $\Delta_t = \|\mathbf{v}_t - \mathbf{x}^*\|_{\mathbf{P}_\lambda^\dagger}^2 + \frac{1}{\tilde{\mu}}\|\mathbf{y}_t - \mathbf{x}^*\|^2 = \mathbf{r}_t + \frac{1}{\tilde{\mu}}\|\mathbf{y}_t - \mathbf{x}^*\|^2$, we conclude that

$$\mathbb{E}[\Delta_{t+1}] \leq \left(1 - \frac{1}{2}\sqrt{\frac{\tilde{\mu}}{\tilde{\nu}}}\right) \cdot \mathbb{E}\left[\mathbf{r}_t^2 + \frac{1}{\tilde{\mu}}\|\mathbf{y}_t - \mathbf{x}^*\|^2\right] = \left(1 - \frac{1}{2}\sqrt{\frac{\tilde{\mu}}{\tilde{\nu}}}\right) \cdot \mathbb{E}[\Delta_t].$$

□

A.2 Proof of Lemma 2.4

Proof of Lemma 2.4. Recall that $1 \leq \nu \leq 1/\mu$, which implies $\bar{\rho} = \sqrt{\mu/\nu} \leq 1/\nu$. Moreover, $\frac{c}{\nu} \leq \eta \leq \frac{1}{\nu} \leq 1$ and $\rho \leq c\bar{\rho} \leq c/\nu \leq \eta$.

(a) Then,

$$\nu \leq \frac{1}{2\eta} \leq \frac{1}{\rho + \eta(1-\rho)} = \tilde{\nu}$$

and

$$\tilde{\mu} = \frac{c^2\bar{\rho}^2}{\rho + \eta(1-\rho)} \leq \frac{c^2\bar{\rho}^2}{\eta} = \frac{c}{\eta}c\bar{\rho}^2 \leq \nu c\bar{\rho}^2 = \mu c \leq \mu.$$

(b) Note that the choice of $\tilde{\mu}$ and $\tilde{\nu}$ and the statement of Lemma 2.3 implies

$$\beta = 1 - \rho, \quad \gamma = 1 + \frac{\eta}{\rho} - \eta, \quad \text{and} \quad \alpha = \frac{\rho}{1 + \rho}. \quad (\text{A.5})$$

Let $\mathbf{m}_t := \frac{\beta(1-\alpha)}{\gamma-1}(\mathbf{v}_t - \mathbf{y}_t)$ for $t \geq 0$. Let's check that then it satisfies the recurrence relation for \mathbf{m}_t . Indeed, from the first equation of (2.2),

$$\mathbf{x}_t - \mathbf{v}_t = (1 - \alpha)(\mathbf{y}_t - \mathbf{v}_t),$$

and then, from the last two equations of (2.2),

$$\begin{aligned} \mathbf{v}_{t+1} - \mathbf{y}_{t+1} &= (\beta\mathbf{v}_t + (1-\beta)\mathbf{x}_t - \gamma\tilde{\mathbf{w}}_t) - (\mathbf{x}_t - \tilde{\mathbf{w}}_t) \\ &= \beta(\mathbf{v}_t - \mathbf{x}_t) - (\gamma-1)\tilde{\mathbf{w}}_t \\ &= \beta(1-\alpha)(\mathbf{v}_t - \mathbf{y}_t) - (\gamma-1)\tilde{\mathbf{w}}_t \\ &= (\gamma-1)(\mathbf{m}_t - \tilde{\mathbf{w}}_t). \end{aligned}$$

By combining the above result with (A.5), we have

$$\mathbf{m}_{t+1} = \frac{\beta(1-\alpha)}{\gamma-1}(\mathbf{v}_{t+1} - \mathbf{y}_{t+1}) = \beta(1-\alpha)(\mathbf{m}_t - \tilde{\mathbf{w}}_t) = \frac{1-\rho}{1+\rho}(\mathbf{m}_t - \tilde{\mathbf{w}}_t).$$

For the update of \mathbf{x}_{t+1} , from (2.2), the definition of \mathbf{m}_t , and (A.5), we have

$$\mathbf{x}_{t+1} = \mathbf{y}_{t+1} + \alpha(\mathbf{v}_{t+1} - \mathbf{y}_{t+1}) = (\mathbf{x}_t - \tilde{\mathbf{w}}_t) + \frac{\alpha(\gamma-1)}{\beta(1-\alpha)}\mathbf{m}_{t+1} = \mathbf{x}_t - \tilde{\mathbf{w}}_t + \eta\mathbf{m}_{t+1}.$$

This concludes the proof of Lemma 2.4. □

B Regularized DPPs: Proof of Lemma 3.6

Proof of Lemma 3.6. To bound the term $\mathbb{E}[(\mathbf{I} + \frac{m}{k\lambda} \mathbf{A}_{S_{\text{DPP}}}^\top \mathbf{A}_{S_{\text{DPP}}})^{-1}]$ for $S_{\text{DPP}} \sim \text{DPP}(\frac{m}{\lambda(m-k)} \mathbf{A} \mathbf{A}^\top + \frac{k}{m-k} \mathbf{I})$, we first introduce the following notion of Regularized DPP (R-DPP). We then show that our DPP sample is equivalent to an R-DPP (in distribution) in Lemma B.2.

Definition B.1 (Regularized DPP, Definition 2 of [DLM20]). *Given matrix $\mathbf{A} \in \mathbb{R}^{m \times n}$, let \mathbf{a}_i^\top denote its i th row. For a sequence $p = (p_1, \dots, p_m) \in [0, 1]^m$ and $\lambda > 0$, define $\text{R-DPP}_p(\mathbf{A}, \lambda)$ as a distribution over $S \subseteq [m]$ such that*

$$\Pr\{S\} = \frac{\det(\mathbf{A}_S^\top \mathbf{A}_S + \lambda \mathbf{I})}{\det(\sum_i p_i \mathbf{a}_i \mathbf{a}_i^\top + \lambda \mathbf{I})} \cdot \prod_{i \in S} p_i \cdot \prod_{i \notin S} (1 - p_i).$$

Lemma B.2 (Lemma 7 in [DLM20]). *Given $\mathbf{A} \in \mathbb{R}^{m \times n}$, $\lambda > 0$ and $p \in [0, 1]^m$, denote $\mathbf{D}_p := \text{diag}(p)$ and $\tilde{\mathbf{D}} := \mathbf{D}_p(\mathbf{I} - \mathbf{D}_p)^{-1}$, then we have*

$$\text{R-DPP}_p(\mathbf{A}, \lambda) = \text{DPP}(\tilde{\mathbf{D}} + \lambda^{-1} \tilde{\mathbf{D}}^{1/2} \mathbf{A} \mathbf{A}^\top \tilde{\mathbf{D}}^{1/2})$$

which means that the R-DPP is equivalent to a DPP from Definition 3.3.

According to Lemma B.2, by choosing $p = (\frac{k}{m}, \dots, \frac{k}{m})$ we have $\text{DPP}(\frac{m}{\lambda(m-k)} \mathbf{A} \mathbf{A}^\top + \frac{k}{m-k} \mathbf{I}) = \text{R-DPP}_p(\mathbf{A}, \frac{k}{m} \bar{\lambda})$, which shows that this DPP can be equivalently viewed as an R-DPP. For an R-DPP we have the following bound.

Lemma B.3 (Lemma 11 in [DLM20]). *For $S \sim \text{R-DPP}_p(\mathbf{A}, \lambda)$ and $p \in [0, 1]^m$,*

$$\mathbb{E} \left[(\mathbf{A}_S^\top \mathbf{A}_S + \lambda \mathbf{I})^{-1} \right] \preceq \left(\sum_i p_i \mathbf{a}_i \mathbf{a}_i^\top + \lambda \mathbf{I} \right)^{-1}.$$

By applying Lemma B.3 to $S_{\text{DPP}} \sim \text{R-DPP}_p(\mathbf{A}, \frac{k}{m} \bar{\lambda})$ where $p = (\frac{k}{m}, \dots, \frac{k}{m})$ we have

$$\mathbb{E} \left[\left(\mathbf{I} + \frac{m}{k\bar{\lambda}} \mathbf{A}_{S_{\text{DPP}}}^\top \mathbf{A}_{S_{\text{DPP}}} \right)^{-1} \right] \preceq \frac{k\bar{\lambda}}{m} \left(\sum_i p_i \mathbf{a}_i \mathbf{a}_i^\top + \frac{k\bar{\lambda}}{m} \mathbf{I} \right)^{-1} = \bar{\lambda} (\mathbf{A}^\top \mathbf{A} + \bar{\lambda} \mathbf{I})^{-1}.$$

□

C Analysis of SymFHT: Proof of Theorem 5.1

Before we analyze the proposed SymFHT algorithm, we first define the Hadamard matrix and state the standard FHT (Fast Hadamard Transform) algorithm as follows.

Definition C.1 (Hadamard matrix). *For $n = 2^m$, we define Hadamard matrix as: $\mathbf{H}_1 = 1$, and for $m \geq 1$,*

$$\mathbf{H}_n = \begin{bmatrix} \mathbf{H}_{n/2} & \mathbf{H}_{n/2} \\ \mathbf{H}_{n/2} & -\mathbf{H}_{n/2} \end{bmatrix} \in \mathbb{R}^{n \times n}.$$

Algorithm 4 Fast Hadamard Transform (FHT)

```

1: function FHT(A)                                     ▷ Input:  $n \times d$  matrix  $\mathbf{A} = [\mathbf{a}_1, \dots, \mathbf{a}_d]$ .
2:   for  $i = 1, 2, \dots, d$  do
3:     Compute  $\mathbf{x}_i \leftarrow \text{FHT}(\mathbf{a}_i[n/2 : n] + \mathbf{a}_i[1 : n/2])$            ▷ Recursive call.
4:     Compute  $\mathbf{y}_i \leftarrow \text{FHT}(\mathbf{a}_i[n/2 : n] - \mathbf{a}_i[1 : n/2])$            ▷ Recursive call.
5:     Compute  $\tilde{\mathbf{a}}_i \leftarrow [\mathbf{x}_i^\top, \mathbf{y}_i^\top]^\top$ 
6:   end for
7:   return  $[\tilde{\mathbf{a}}_1, \dots, \tilde{\mathbf{a}}_d]$                                        ▷ Computes  $\mathbf{H}_n \mathbf{A}$ .
8: end function

```

Denote $\mathcal{T}_{\text{FHT}}(n, d)$ as the FLOPs it takes to compute $\text{FHT}(\mathbf{A})$ for $\mathbf{A} \in \mathbb{R}^{n \times d}$. Notice that if we set $d = 1$ in Algorithm 4, then it recovers the vector version of FHT, in this case by recursion we have $\mathcal{T}_{\text{FHT}}(n, 1) = 2\mathcal{T}_{\text{FHT}}(n/2, 1) + n = n \log n$. For standard matrix cases, we have $\mathcal{T}_{\text{FHT}}(n, d) = d \cdot \mathcal{T}_{\text{FHT}}(n, 1) = nd \log n$.

In CD++ (Algorithm 3), we need to compute $\mathbf{Q}\mathbf{A}\mathbf{Q}^\top$ for a symmetric matrix \mathbf{A} , where $\mathbf{Q} = \mathbf{H}_n \mathbf{D}$, for $\mathbf{D} = \frac{1}{\sqrt{n}} \text{diag}(d_1, \dots, d_n)$ and d_i are independent random ± 1 signs (Rademacher variables). In order to construct this transformation, we can naively apply FHT twice to matrix $\mathbf{D}\mathbf{A}\mathbf{D}$ and have $\mathbf{Q}\mathbf{A}\mathbf{Q}^\top = \text{FHT}(\text{FHT}(\mathbf{D}\mathbf{A}\mathbf{D})^\top)$. Notice that the cost of applying FHT to an $n \times n$ matrix is $n^2 \log n$, thus this naive method takes $2n^2 \log n$ FLOPs. However, this method does not take the symmetry of \mathbf{A} into account. We improve on this with our proposed SymFHT (Algorithm 2).

Proof of Theorem 5.1. Denote $\mathbf{H} := \mathbf{H}_{n/2}$. Then, for symmetric matrix \mathbf{A} we have the following:

$$\mathbf{H}_n \mathbf{A} \mathbf{H}_n = \begin{bmatrix} \mathbf{H} & \mathbf{H} \\ \mathbf{H} & -\mathbf{H} \end{bmatrix} \begin{bmatrix} \mathbf{A}_{11} & \mathbf{A}_{12} \\ \mathbf{A}_{12}^\top & \mathbf{A}_{22} \end{bmatrix} \begin{bmatrix} \mathbf{H} & \mathbf{H} \\ \mathbf{H} & -\mathbf{H} \end{bmatrix} = \begin{bmatrix} \mathbf{C}_{11} + \mathbf{C}_{21} & \mathbf{C}_{12} + \mathbf{C}_{22} \\ \mathbf{C}_{12}^\top + \mathbf{C}_{22}^\top & \mathbf{C}_{12} - \mathbf{C}_{22} \end{bmatrix}$$

where matrices \mathbf{C}_{11} , \mathbf{C}_{12} and \mathbf{C}_{22} are given by

$$\begin{aligned} \mathbf{C}_{11} &= \mathbf{H}(\mathbf{A}_{11} + \mathbf{A}_{12}^\top)\mathbf{H} & \mathbf{C}_{12} &= \mathbf{H}(\mathbf{A}_{11} - \mathbf{A}_{12})\mathbf{H} \\ \mathbf{C}_{21} &= \mathbf{H}(\mathbf{A}_{12} + \mathbf{A}_{22})\mathbf{H} & \mathbf{C}_{22} &= \mathbf{H}(\mathbf{A}_{12}^\top - \mathbf{A}_{22})\mathbf{H} \end{aligned}$$

Thus if we pre-compute $\mathbf{B}_{11} := \mathbf{H}\mathbf{A}_{11}\mathbf{H}$, $\mathbf{B}_{12} := \mathbf{H}\mathbf{A}_{12}\mathbf{H}$, $\mathbf{B}_{22} = \mathbf{H}\mathbf{A}_{22}\mathbf{H}$, then

$$\begin{aligned} \mathbf{C}_{11} &= \mathbf{B}_{11} + \mathbf{B}_{12}^\top & \mathbf{C}_{12} &= \mathbf{B}_{11} - \mathbf{B}_{12} \\ \mathbf{C}_{21} &= \mathbf{B}_{12} + \mathbf{B}_{22} & \mathbf{C}_{22} &= \mathbf{B}_{12}^\top - \mathbf{B}_{22} \end{aligned}$$

We note that due to symmetry, we do not need to compute $\mathbf{H}\mathbf{A}_{21}\mathbf{H} = \mathbf{H}\mathbf{A}_{12}^\top\mathbf{H}$. When we compute \mathbf{B}_{11} and \mathbf{B}_{22} , since both \mathbf{A}_{11} and \mathbf{A}_{22} are also symmetric, we can compute them recursively, i.e., $\mathbf{B}_{11} = \text{SymFHT}(\mathbf{A}_{11})$, $\mathbf{B}_{22} = \text{SymFHT}(\mathbf{A}_{22})$. However when we compute \mathbf{B}_{12} , since \mathbf{A}_{12} is no longer symmetric, we can no longer use the same scheme; instead, we can apply standard FHT twice to this smaller matrix, i.e., $\mathbf{B}_{12} = \text{FHT}(\text{FHT}(\mathbf{A}_{12}^\top)^\top)$. Notice that the costs for computing \mathbf{C}_{11} , \mathbf{C}_{12} , \mathbf{C}_{21} and \mathbf{C}_{22} are all $(n/2)^2 = n^2/4$. In addition, we need to compute $\mathbf{C}_{11} + \mathbf{C}_{21}$, $\mathbf{C}_{12} + \mathbf{C}_{22}$ and $\mathbf{C}_{12} - \mathbf{C}_{22}$. These sum up to $7n^2/4$ FLOPs. Thus, the cost of SymFHT is governed by the following recursive inequality:

$$\begin{aligned} \mathcal{T}_{\text{SymFHT}}(n) &\leq 2\mathcal{T}_{\text{SymFHT}}(n/2) + 2\mathcal{T}_{\text{FHT}}(n/2, n/2) + 7n^2/4 \\ &\leq 2\mathcal{T}_{\text{SymFHT}}(n/2) + 2(n/2)^2 \log(n/2) + 7n^2/4 \\ &= 2\mathcal{T}_{\text{SymFHT}}(n/2) + 2(n/2)^2(\log n + 2.5) \\ &\leq \frac{1}{2}n^2(2.5 + \log n) \cdot \left(1 + \frac{1}{2} + \frac{1}{2^2} + \dots\right) \leq n^2(2.5 + \log n) \end{aligned}$$

where we use the fact that $\mathcal{T}_{\text{FHT}}(n, n) = n^2 \log n$ and that $n \geq 4$. Compared to the naïve method, our algorithm SymFHT reduces the FLOPs by about a half. \square

D Further Numerical Experiments

In this section we provide the details for our experimental setup, and we give the results for the test matrices and experiments not included in Section 6. We also carry out additional experiments evaluating the effect of Tikhonov regularization on the Kaczmarz projection steps. The code for our experiments is available at <https://github.com/EdwinYang7/kaczmarz-plusplus>.

First, we discuss the specifics of the construction of our test matrices. Recall that each of our test matrices is an $n \times n$ PSD matrix \mathbf{A} with $n = 4096$, and our task is solving a linear system $(\mathbf{A} + \phi \mathbf{I})\mathbf{x} = \mathbf{b}$ where we choose $\phi = 0.001$ and generate \mathbf{b} from the standard normal distribution. Note that we choose n to be a power of 2 simply for the convenience of implementing randomized Hadamard transform (RHT). In general this is not necessary, since we can still implement it by finding the closest power of 2 larger than n , enlarging the matrix to that dimension by padding with 0 entries, and truncating back to the original dimension at the end.

We consider the following two classes of test matrices.

1. Synthetic Low-Rank Matrices. To validate our theories on the effect of the number of large outlying eigenvalues, we carry out experiments on synthetic benchmark matrices using the function `make_low_rank_matrix` from Scikit-learn [PVG⁺11], which provides random matrices with a bell-shaped spectrum, motivated by data in computer vision and natural language processing. As specified in Scikit-learn, the singular value profile of a matrix $\Phi \in \mathbb{R}^{n_{\text{samples}} \times n_{\text{features}}}$ generated this way is: $(1 - \text{tail_strength}) \cdot \exp(-(i/\text{effective_rank})^2)$ for the top `effective_rank` singular values, and $\text{tail_strength} \cdot \exp(i/\text{effective_rank})$ for the remaining ones. We set parameters $n_{\text{samples}} = n_{\text{features}} = n$ and choose parameter `effective_rank` among the four values $\{25, 50, 100, 200\}$. Note that parameter `effective_rank` is approximately the number of singular vectors required to explain most of the data by linear combinations. It can be viewed as “the number of large singular values k ” in our theory, and is also roughly the number of steps needed for Krylov-type methods to construct a good Krylov subspace. Parameter `tail_strength`, which captures the relative importance of the fat noisy tail of the spectrum, is set to 0.01. With this matrix Φ constructed, we let $\mathbf{A} = \Phi \Phi^\top$ which defines the PSD linear system. This leads to a total of 4 test matrices.

2. Kernel Matrices from Machine Learning. To evaluate our algorithm in a practical setting that naturally exhibits large outlying eigenvalues, we consider applying kernel transformation to four real-world datasets (Abalone and Phoneme from OpenML [VvRBT13], California_housing and Covtype from Scikit-learn [PVG⁺11]). We truncate each dataset to its first n rows to get matrix $\Phi \in \mathbb{R}^{n \times m}$. For $(i, j) \in [n] \times [n]$, we define the kernel matrix $\mathbf{A} \in \mathcal{S}_d^+$ so that $\mathbf{A}_{ij} = \mathcal{K}(\Phi_i, \Phi_j)$ where Φ_i, Φ_j are the i -th and j -th rows of Φ , respectively, and \mathcal{K} is a kernel function. We consider two types of kernel functions: Gaussian, $\mathcal{K}(\Phi_i, \Phi_j) = \exp(-\gamma \|\Phi_i - \Phi_j\|^2)$, and Laplacian, $\mathcal{K}(\Phi_i, \Phi_j) = \exp(-\gamma \|\Phi_i - \Phi_j\|)$. For both choices, we set the width parameter γ among two values, $\{0.1, 0.01\}$. This leads to four different test matrices for each of the four datasets, giving a total of 16 matrices.

D.1 Testing Acceleration and Block Memoization

In this section we test the effect of both the adaptive acceleration scheme as well as the block memoization technique used in our methods (see Figure 1 in Section 6 and Figure 3 below). For

all tasks, we used variants of CD++ (Algorithm 3), since it is designed specifically for solving PSD linear systems. Recall that CD++ can also be viewed as the dual algorithm of Kaczmarz++ (Algorithm 1) in the sense that instead of sampling principal submatrices of \mathbf{A} , it is sampling rows of matrix Φ . So, in that sense, these experiments simultaneously provide an evaluation of the convergence properties of Kaczmarz++ (Algorithm 1). We consider four variants of our method, as shown in Table 1, to identify the effect of each component individually. For clarity, we explain their differences below.

- CD: The classical block coordinate descent method, without acceleration or block memoization, but still preprocessed with RHT;
- CD+Accel: Coordinate descent with adaptive acceleration, but without block memoization, i.e., Algorithm 3 modified so that in line 6 we always choose to sample a new block $S \sim \binom{[n]}{s}$, and hence, do not save the Cholesky factors;
- CD+Memo: Coordinate descent with block memoization (but without adaptive acceleration), i.e., Algorithm 3 without lines 14-20, and with $\eta = 0$ (as opposed to $\eta = \frac{s}{2n}$), meaning that we no longer maintain the adaptive momentum term \mathbf{m}_t from line 12;
- Full CD++: Algorithm 3 as given in the pseudocode, equipped with both adaptive acceleration and block memoization.

Throughout this section, we set the sketch size s to be $\{25, 50, 100, 200\}$, and measure the convergence through the residual error defined as $\epsilon_t := \|\mathbf{A}_\phi \mathbf{x}_t - \mathbf{b}\| / \|\mathbf{b}\|$ where $\mathbf{A}_\phi := \mathbf{A} + \phi \mathbf{I}$. For each plot we run all methods 10 times and take an average.

By comparing the curves, we can see that in all cases, adding block memoization slightly worsens the convergence rate (by comparing CD and CD+Memo, or CD+Accel and Full CD++). This is actually suggested by theory, since with block memoization we are essentially not sampling all possible blocks of coordinates, thus reducing the quality of the block sampling distribution. However it is noteworthy that this phenomenon is very insignificant especially when we compare CD+Accel with Full CD++, which suggests that our online block selection scheme (described in Section 5.2) works well, and that $\tilde{O}(n/s)$ blocks are sufficient for fast convergence, matching our theory.

From the plots, we can also see that the adaptive acceleration plays an important role for both CD and CD with block memoization, showing a comparable improvement for both cases. We also observe that the effect of adaptive acceleration is more significant when the sketch size s is smaller - this also aligns with the theory, since for smaller s the tail Demmel condition number $\bar{\kappa}_s$ is larger, thus the effect of acceleration reducing the dependence on $\bar{\kappa}_s$ from second to first power is also more significant.

To conclude, the experiments in this section suggest that both CD with and without block memoization benefit from our adaptive acceleration scheme. Based on this, in next section we will carry out more experiments testing the effect of block memoization; namely, we will test the performance of CD+Accel and Full CD++ alongside Krylov-type methods including CG and GMRES.

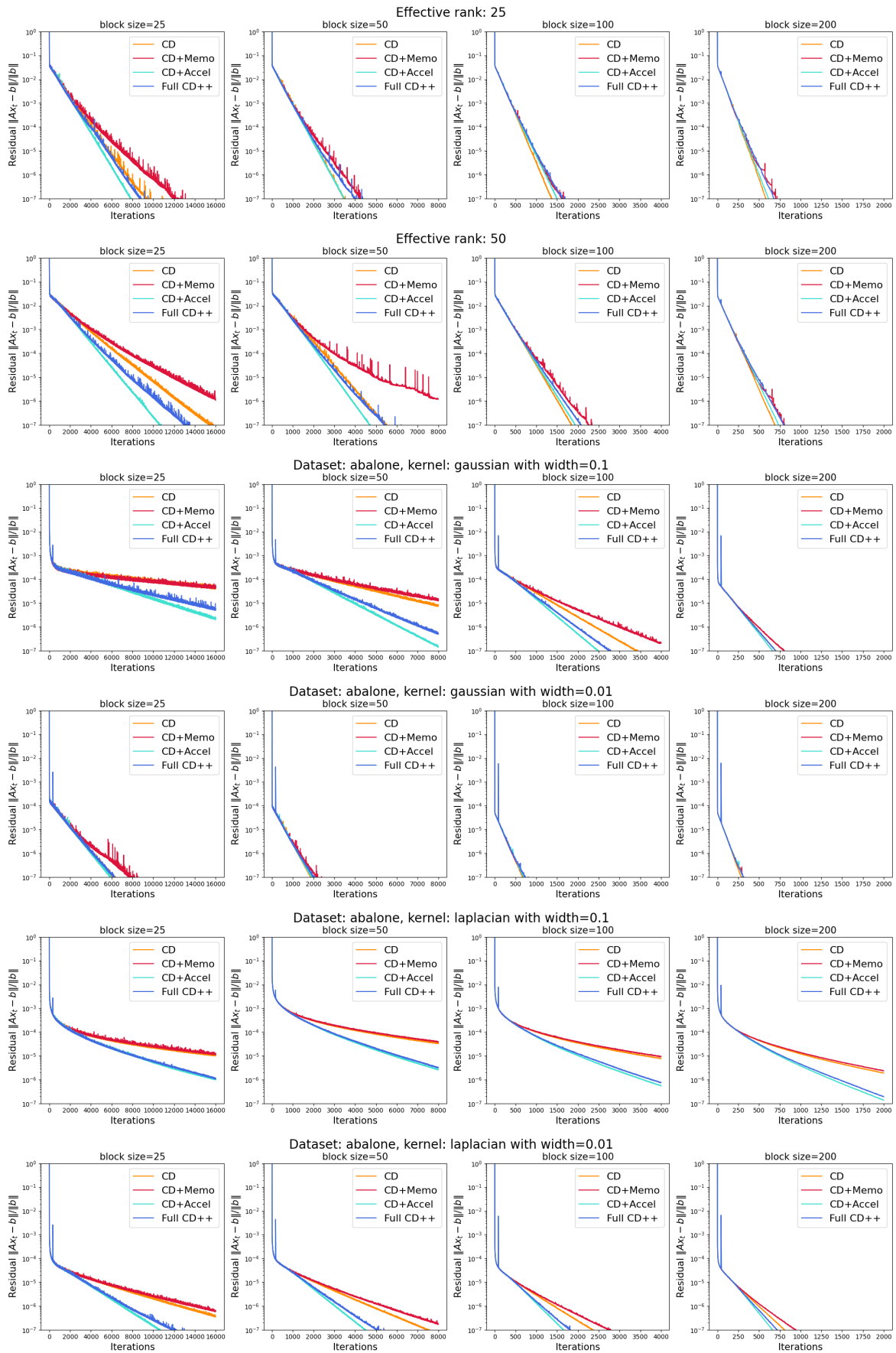


Figure 3: Convergence plots for different variants of CD++ (see Table 1) using four block sizes (continuation of Figure 1). Check <https://github.com/EdwinYang7/kaczmarz-plusplus> for plots on remaining real-world datasets.

D.2 Comparison with Krylov Subspace Methods

Next, we test the convergence of our Full CD++ alongside CD+Accel, against Krylov-type methods, conjugate gradient (CG) and GMRES. In this experiment we count the FLOPs it takes to converge for each method, to showcase the advantages of our methods compared to Krylov-type methods.

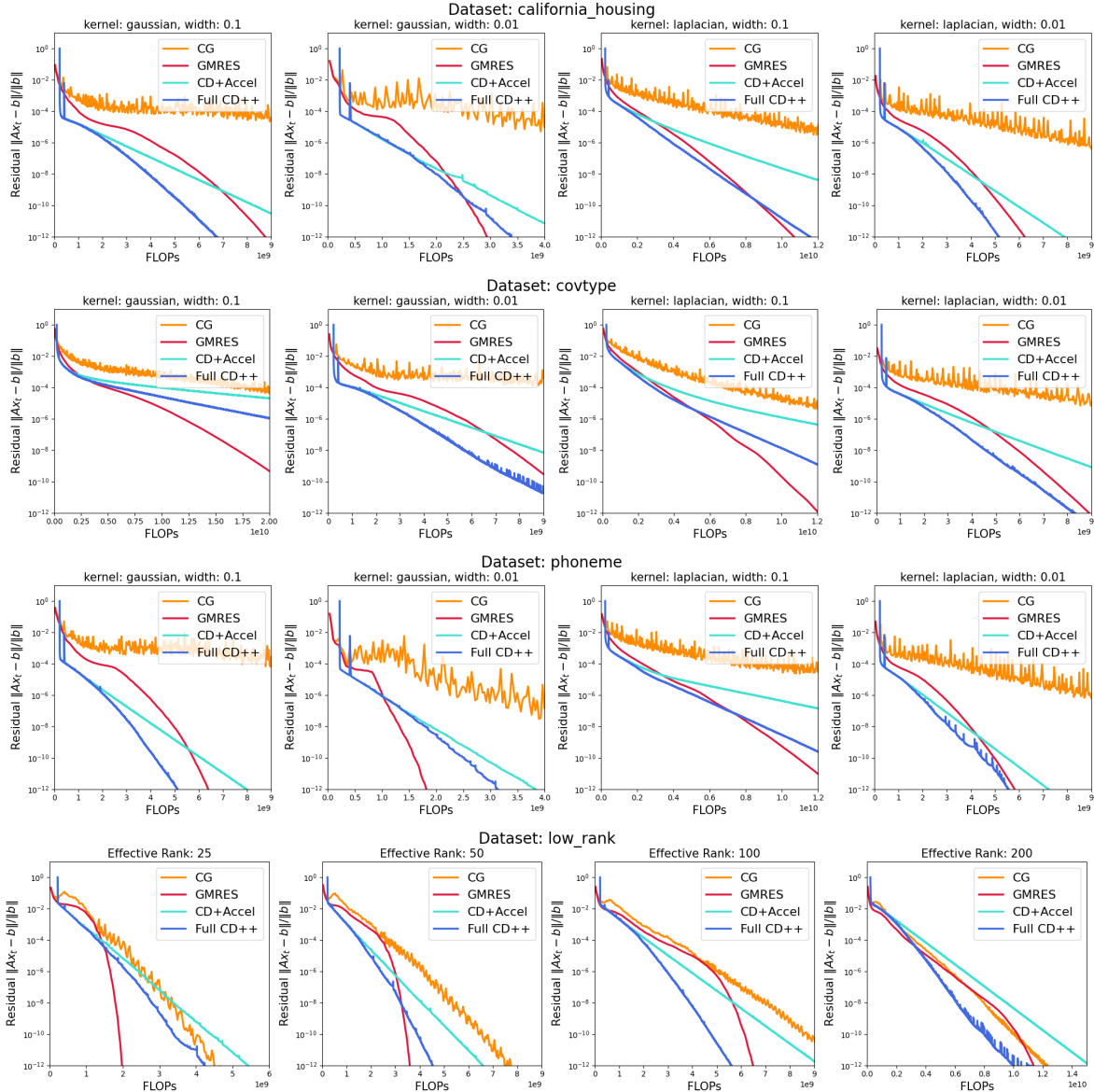


Figure 4: Computational cost comparison, measuring floating point operations (FLOPs) against the normalized residual error (6.1) for Full CD++, alongside baselines CD+Accel, CG, and GMRES (continuation of Figure 2).

For the FLOPs of CG, we look into the source code from [scipy.sparse.linalg](#) and approximate it by $2n^2 + 11n$ per iteration. For the FLOPs counting of GMRES, we look into the source code from [pyang.krylov](#) and approximate it by $2n^2T + 4nT(T + 1)$, where T is the number of iterations. For the FLOPs counting of our methods (CD+Accel, Full CD++), we maintain a counter for FLOPs for each iteration, which includes both the cases of using (Full CD++) and not using (CD+Accel)

Problem			CG		GMRES		CD++	
Dataset	Kernel	Width	1e-4	1e-8	1e-4	1e-8	1e-4	1e-8
Abalone	Gaussian	0.1	7.63e9	3.06e10	1.47e9	5.17e9	4.64e8	3.26e9
		0.01	1.88e9	6.89e9	8.50e8	1.75e9	2.97e8	2.11e9
	Laplacian	0.1	8.64e9	3.22e10	2.72e9	8.14e9	2.22e9	8.13e9
		0.01	1.11e9	1.37e10	5.41e8	4.11e9	2.40e8	3.09e9
Phoneme	Gaussian	0.1	7.80e9	3.29e10	1.79e9	4.98e9	4.86e8	3.23e9
		0.01	3.70e8	4.23e9	3.37e8	1.33e9	2.23e8	1.80e9
	Laplacian	0.1	7.22e9	3.73e10	2.29e9	8.46e9	1.65e9	8.96e9
		0.01	2.49e9	1.41e10	7.81e8	3.97e9	2.80e8	3.10e9
California Housing	Gaussian	0.1	2.45e9	3.27e10	1.02e9	6.14e9	2.40e8	3.88e9
		0.01	2.15e9	9.51e9	5.75e8	2.18e9	2.27e8	1.99e9
	Laplacian	0.1	5.44e9	2.34e10	2.04e9	6.85e9	1.52e9	6.39e9
		0.01	1.31e9	1.36e10	5.75e8	4.15e9	2.40e8	3.06e9
Covtype	Gaussian	0.1	1.65e10	5.55e10	4.87e9	1.70e10	5.71e9	3.64e10
		0.01	9.31e9	3.87e10	2.00e9	7.69e9	9.78e8	5.66e9
	Laplacian	0.1	6.79e9	2.24e10	3.23e9	8.34e9	2.85e9	1.03e10
		0.01	3.60e9	2.37e10	1.23e9	5.95e9	4.60e8	4.56e9
Synthetic Low-Rank	Effective rank = 25		1.68e9	3.26e9	1.44e9	1.83e9	1.31e9	2.79e9
	Effective rank = 50		2.59e9	5.17e9	2.43e9	3.26e9	1.53e9	3.21e9
	Effective rank = 100		3.16e9	6.89e9	2.65e9	5.67e9	1.91e9	3.89e9
	Effective rank = 200		3.26e9	8.00e9	2.75e9	8.34e9	2.92e9	6.10e9

Table 2: Comparison of the FLOPs needed to achieve given error threshold, $\epsilon \in \{10^{-4}, 10^{-8}\}$, for different algorithms. Bold values indicate the best performance for a given error threshold.

block memoization. Specifically, for Full CD++ which leverages block memoization, if a new block is sampled, then we do the Cholesky factorization and increase the FLOPs by $s^3/3$, where s is the block size; if we sample from the already sampled set of blocks \mathcal{B} , then Cholesky factorization is not needed and this cost is omitted. Notice that for CD+Accel and Full CD++, there is a pre-processing step of applying the RHT which takes extra FLOPs. We count them by following Appendix C, and this is reflected in the plots, since the convergence curves of our methods are shifted by the cost of the RHT. Here, we take advantage of our fast SymFHT implementation (Algorithm 2), which reduces that cost by half. Throughout the section, we choose the block size $s = 200$, which tends to work well for the size of our test matrices. Further optimizing the block size, or choosing it dynamically, is an interesting direction for future work. For each plot, we run CD+Accel and Full CD++ 5 times and take average to reduce the noise.

From the experiments (Figure 4), we can see that CG converges very slowly and is not comparable with other methods. By comparing CD+Accel and Full CD++, we can see that the block memoization technique gives a significant improvement in FLOPs, since Full CD++ successfully reduces the expensive Cholesky factorization step. This improvement is more significant if we are running more iterations (i.e., aiming for higher accuracy). By comparing Full CD++ and GMRES, we can see that in most cases Full CD++ performs better in the “low to medium accuracy level”, while GMRES sometimes beats Full CD++ in the “high accuracy level”.

For example, for the abalone dataset with Gaussian kernel with width=0.01, GMRES starts to perform better after the residual reaches 10^{-7} . However, we note that for abalone, phoneme and california.housing dataset with Gaussian kernel with width=0.1, or with Laplacian kernel with width=0.01, our Full CD++ outperforms GMRES even when the residual reaches 10^{-12} . These phenomena are dependent on the spectrum (especially the top eigenvalues) of matrix $\mathbf{A} + \phi\mathbf{I}$, which is reflected in the different choices of kernel and width.

In Table 2 we show the FLOPs it takes for different methods (CG, GMRES, CD+Accel and Full CD++) to achieve the given accuracy in detail. Here we set $\epsilon = 10^{-4}$ as the mid-level accuracy and $\epsilon = 10^{-8}$ as the high-level accuracy. For mid-level accuracy, we can see that Full CD++ outperforms GMRES in 18 out of 20 tasks, showing that our method converges super fast at early stages. For high-level accuracy, we can see that Full CD++ still outperforms GMRES at 14 out of 20 tasks.

To conclude, the experiments in this section show that in the measurement of FLOPs, our CD++ outperforms Krylov methods including CG and GMRES in almost all mid-level accuracy tasks, as well as most high-level accuracy tasks.

D.3 Testing Regularization in Projection

In this section, we test the effect of explicitly adding regularization to the projection step in Kaczmarz++/CD++ (parameter λ in Algorithm 3). We test this experiments on our Full CD++ method with $\lambda = \{1e-2, 1e-4, 1e-6, 1e-8, 1e-10, 0\}$, where in the case of $\lambda = 1e-8$, this recovers the Full CD++ used in the remaining experiments. As we can see in Figure 5 adding this regularization term does not have a significant effect on the convergence rate of Full CD++ (we do not include the plots for the remaining 3 real-world datasets, since they all show the same phenomena). This shows that adding regularization does not sacrifice the convergence rate. Recall that regularization has the benefit of making the computation of the Cholesky factors more stable: in the case where we solve a positive semidefinite (i.e., $\phi = 0$) linear system the Cholesky factorization step can be potentially numerically unstable if the block matrix $\mathbf{A}_{S,S}$ is singular. Thus, we recommend using CD++ with a small but positive λ to ensure numerical stability.

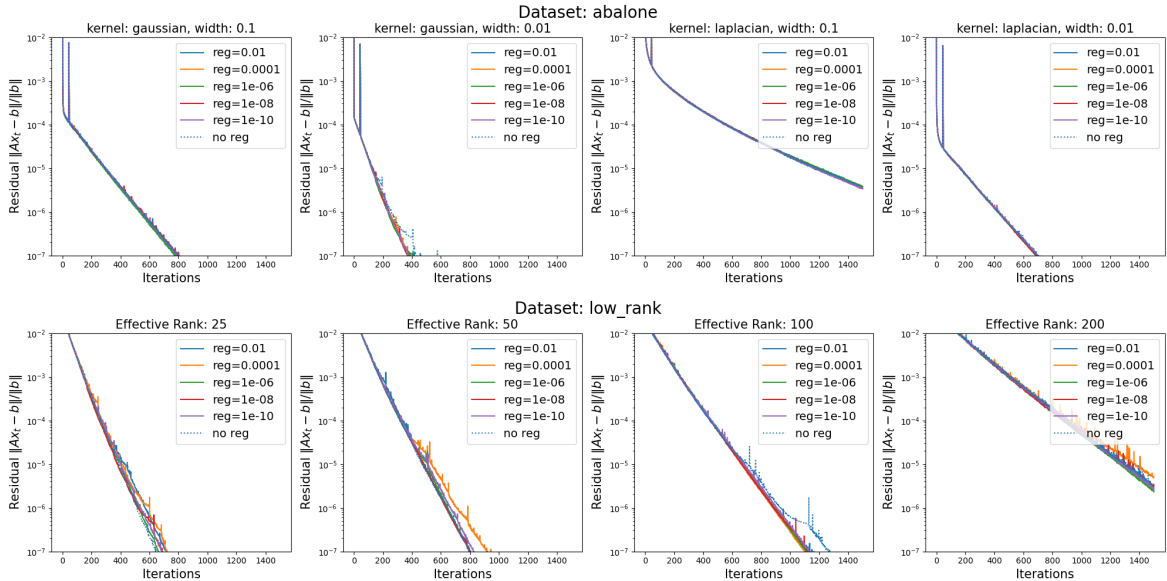


Figure 5: Convergence plots showing the stability of CD++ with respect to the choice of Tikhonov regularization parameter λ in the inner step of CD++. Check <https://github.com/EdwinYang7/kaczmarz-plusplus> for plots on remaining real-world datasets.